Calibration of the oxygen and clumped isotope thermometers for (proto-)dolomite based on synthetic and natural carbonates

Inigo A. Müller[a,b,*], Juan D. Rodriguez-Blanco[c,e], Julian-Christopher Storck[b], Gabriela Santilli do Nascimento[b], Tomaso R.R. Bontognali[g,h], Crisogono Vasconcelos[b], Liane G. Benning[d,e,f], Stefano M. Bernasconi[b]

[a] Faculty of Geosciences, Utrecht University, Utrecht, Netherlands
[b] Department of Earth Sciences, ETH Zurich, Zurich, Switzerland
[c] iCRAG Department of Geology, School of Natural Sciences, Trinity College Dublin, Dublin, Ireland
[d] German Research Centre for Geosciences, GFZ, Potsdam, Germany
[e] School of Earth and Environment, University of Leeds, Leeds, UK
[f] Department of Geology, Free University of Berlin, Berlin, Germany
[g] Space Exploration Institute (SPACE-X), Neuchatel, Switzerland
[h] University of Basel, Department of Environmental Sciences, Basel, Switzerland

ARTICLE INFO

ABSTRACT

Dolomite is a very common carbonate mineral in ancient sediments, but is rarely found in modern environments. Because of the difficulties in precipitating dolomite in the laboratory at low temperatures, the controls on its formation are still debated after more than two centuries of research. Two important parameters to constrain the environment of dolomitization are the temperature of formation and the oxygen isotope composition of the fluid from which it precipitated. Carbonate clumped isotopes (expressed with the parameter Δ_{47}) are increasingly becoming the method of choice to obtain this information. However, whereas many clumped isotope studies treated dolomites the same way as calcite, some recent studies observed a different phosphoric acid fractionation for Δ_{47} during acid digestion of dolomite compared to calcite. This causes additional uncertainties in the Δ_{47} temperature estimates for dolomites analyzed in different laboratories using different acid digestion temperatures.

To tackle this problem we present here a (proto-)dolomite-specific Δ_{47}-temperature calibration from 25 to 1100 °C for an acid reaction temperature of 70 °C and anchored to widely available calcite standards. For the temperature range 25 to 220 °C we obtain a linear Δ_{47}-T relationship based on 289 individual measurements with R^2 of 0.864:

$$\Delta_{47\ CDES\ 70°C} = 0.0428 \pm 0.0020 \times \left(\frac{10^6}{T^2}\right) + 0.1481 \pm 0.0160 \text{ (T in Kelvin)}$$

When including two isotopically scrambled dolomites at 1100 °C, the best fit is obtained with a third order polynomial temperature relationship (R^2 = 0.924):

$$\Delta_{47\ CDES\ 70°C}(‰) = -0.0002 \times \left(\frac{10^6}{T^2}\right)^3 + 0.0041 \times \left(\frac{10^6}{T^2}\right)^2 + 0.0115 \times \left(\frac{10^6}{T^2}\right) + 0.2218.$$

Applying a calcite Δ_{47}-T relationship produced under identical laboratory conditions results in 3 to 16 °C colder calculated formation temperatures for dolomites (with formation temperature from 0 to 100 °C) than using the (proto-)dolomite specific calibration presented here.

For the synthetic samples formed between 70 and 220 °C we also determined the temperature dependence of the oxygen isotope fractionation relative to the water. Based on the similarity between our results and two other recent studies (Vasconcelos et al., 2005 and Horita, 2014) we propose that a combination of the three datasets represents the most robust calibration for (proto-)dolomite formed in a wide temperature range from 25 to 350 °C.

* Corresponding author at: Faculty of Geosciences, Utrecht University, Utrecht, Netherlands.
E-mail address: i.a.muller@uu.nl (I.A. Müller).

$$10^3\alpha_{CaMg-carbonates-Water} = 2.9923 \pm 0.0557 \times \left(\frac{10^6}{T^2}\right) - 2.3592 \pm 0.4116$$

Because of the uncertainties in the phosphoric acid oxygen and clumped isotope fractionation for (proto-) dolomite, we promote the use of three samples that are available in large amounts as possible inter-laboratory reference material for oxygen and clumped isotope measurements. A sample of the middle Triassic San Salvatore dolomite from southern Switzerland, the NIST SRM 88b dolomite standard already reported in other Δ_{47} studies and a lacustrine Pliocene dolomite from La Roda (Spain).

This study demonstrates the necessity to apply (proto-)dolomite specific Δ_{47}-T relationships for accurate temperature estimates of dolomite formation, ideally done at identical acid digestion temperatures to avoid additional uncertainties introduced by acid digestion temperature corrections. In addition, the simultaneous analyses of dolomite reference material will enable a much better comparison of published dolomite clumped and oxygen isotope data amongst different laboratories.

1. Introduction

The formation of dolomite ($Ca,Mg(CO_3)_2$) in nature has been subject to extensive research for more than two centuries. In spite of all the efforts it remains unclear how this mineral forms at Earth surface conditions and why it is so abundant during certain time intervals in the geological past (Land, 1985; Given and Wilkinson, 1987; Spencer and Hardie, 1990; Chai et al., 1995; Hardie, 1996; Holland et al., 1996; Wright, 1997; Land, 1998; Burns et al., 2000; Warren, 2000). In modern environments only few places of active (proto-)dolomite formation at the surface are known and in most of these cases microorganisms have been shown to play an active or passive role (e.g. Vasconcelos and McKenzie, 1997; Wright, 1999; Bontognali et al., 2010; Brauchli et al., 2016). However, the amount and geographic extent of recent dolomite formation is only very small compared to the amounts that were formed during specific time intervals in the past, such as the Triassic (Berra et al., 2010) or the Cryogenian (Hood et al., 2011; Hood and Wallace, 2012). Such episodes of widespread dolomite formation were followed and preceded by time intervals where limestone ($CaCO_3$) was the dominant carbonate sediment. These transitions between dolomite and limestone-rich time intervals in the geological record are thought to be triggered by changes in global seawater chemistry or by changes in the depositional environment (e.g. Hardie, 1996; Holland et al., 1996; McCormack et al., 2018). To improve our models of dolomitization it is crucial to better characterize the temperature of formation and the composition of the fluid responsible for dolomite formation.

Many examples exist where microstructures and fossils in ancient dolomites point to a very early diagenetic formation in shallow seawater or lacustrine environment (e.g. Frisia, 1994; García del Cura et al., 2001; Hood and Wallace, 2012; Huang et al., 2014). In contrast, the absence of such signatures with a rather homogenous micritic matrix can indicate a secondary dolomite formation during early or burial diagenesis following dissolution of a primary carbonate phase or its conversion into well-ordered dolomite at a later stage. Complementary to microscopic methods, geochemical tools such as stable isotopes of oxygen, carbon or strontium were used to gain further insights in the environment or the "parental fluid" in which the mineral precipitated (e.g. Land, 1980; Wilson et al., 1990; Preto et al., 2015).

During the last decade carbonate clumped isotope thermometry evolved as a promising tool to determine formation temperatures of carbonates and the oxygen isotope composition of the fluid source (e.g. Ghosh et al., 2006a, 2006b; Eiler, 2007; Bristow et al., 2011; Ferry et al., 2011; Dale et al., 2014; Millán et al., 2016; Winkelstern and Lohmann, 2016; Rodríguez-Sanz et al., 2017; Suarez et al., 2017; Mangenot et al., 2018; Smeraglia et al., 2018; Leutert et al., 2019). Thus it is now possible to gain important insights on the environment of carbonate mineral formation. Clumped isotope thermometry is a measure of the abundance of the $^{13}C-^{18}O$ bond within the carbonate mineral relative to its stochastic isotope distributions, which is solely temperature dependent. Carbonate clumped isotopes are measured on

the CO_2 gas evolved from the reaction of the carbonate mineral with phosphoric acid as the mass 47 ($^{13}C^{18}O^{16}O$). The clumped isotope composition of carbonates is thus reported in the Δ_{47} notation:

$$\Delta_{47} = ((R^{47}/R^{47*} - 1) - (R^{46}/R^{46*} - 1) - (R^{45}/R^{45*} - 1)) * 1000 \, (‰),$$

where the measured ratios between the m/z 45, 46 and 47 over the most abundant CO_2 isotopologue m/z 44 (R^i) are reported against their stochastic isotope distribution (R^{i*}), which is calculated from the bulk isotope composition of the sample gas ($\delta^{13}C$ and $\delta^{18}O$). The phosphoric acid reaction of the carbonate to CO_2 produces a temperature-dependent isotopic fractionation whose temperature dependence is relatively well constrained for calcite (e.g. Defliese et al., 2015; Murray et al., 2016; Petersen et al., 2019) but not for dolomite. The temperature dependence of this acid fractionation is of high importance as it is common practice to project the Δ_{47} value, derived for laboratory-specific acid reaction temperatures, to an acid digestion temperature of 25 °C. To do so, laboratories correct their data with an acid fractionation correction factor (AFF), derived from studies that reacted the same carbonate powder with phosphoric acid at different temperatures (e.g. Passey et al., 2010; Wacker et al., 2013; Defliese et al., 2015; Murray et al., 2016). This AFF is equal to the offset between the Δ_{47} acid fractionation of the used reaction temperature and a 25 °C reaction enabling a direct comparison to the pioneering clumped isotope studies (Ghosh et al., 2006a, 2006b) and between different laboratories.

For dolomite, however, the temperature dependence of the AFF is still debated. While earlier studies processed their Δ_{47} measurements of different carbonate minerals with the same AFF as for calcite, two recent studies on the temperature dependence of the AFF for dolomite came to contrasting conclusions (Defliese et al., 2015; Murray et al., 2016). Whereas Defliese et al. (2015) observed similar temperature sensitivities for the AFF of dolomite and calcite, Murray et al. (2016) observed a much steeper temperature sensitivity for the AFF of dolomite relative to calcite. In a study on the absolute Δ_{47} acid fractionation at 70 °C acid digestion temperature, Müller et al. (2017a) moreover, observed a significantly smaller acid fractionation for aragonite (0.172 ‰), compared to calcite (0.197 ‰) and dolomite (0.226‰). In this study, Müller et al. (2017a) also determined the acid fractionation for dolomite at 100 °C and observed that at this temperature it is smaller than that of calcite supporting the findings of Murray et al. (2016). Interestingly, the results of Müller et al. (2017a) indicate that the Δ_{47} acid fractionations of dolomite and calcite seems to be identical at about 90 °C acid digestion temperature, the reaction temperature currently used by most clumped isotope laboratories with common acid bath systems for large samples. These inconclusive findings on the Δ_{47} acid fractionation of dolomite at different reaction temperatures can cause large uncertainties on the interpretation of the Δ_{47} based formation temperature of dolomites, especially when comparing studies that use different acid digestion temperatures.

Recently two dolomite-specific Δ_{47}-T calibrations were published (Winkelstern et al., 2016; Bonifacie et al., 2017) with the aim of

eliminating additional uncertainties in the interpretation of dolomite clumped isotope temperatures. The study of Winkelstern et al. (2016) for 75 °C dolomite acid digestion after correction with the new IUPAC parameters for the correction of the ^{17}O abundance (parameters recommended by Daëron et al., 2016 from original studies of Baertschi, 1976; Chang and Li, 1990; Assonov and Brenninkmeijer, 2003; Barkan and Luz, 2005) by Petersen et al. (2019) gives slope a 0.0404 (± 0.0027) and an intercept of 0.240 (± 0.015) a significant change from the original publication which gave a slope of 0.0378 and an intercept of 0.300. This slope is slightly lower than that of other - calcite specific calibrations (the ones corrected for non-linearity effects due to negative backgrounds, reported in the absolute reference frame and using a wider sample temperature range with sufficient replicates, see Fernandez et al., 2017). On the other hand, Bonifacie et al. (2017) for 90 °C acid digestion revealed that the temperature relationship of dolomite is within error of the one of calcite based on a compilation of many different published laboratories carried out in the same study. This proposed universal calibration was also statistically indistinguishable from the one for calcite of Kele et al. (2015), which was produced in our laboratory, before recalculation with the IUPAC parameters. A recalculation of the Kele et al. (2015) by Bernasconi et al. (2018), however, showed that while the slope remained constant, the intercept decreased by 0.038 ‰. Unfortunately the composition of the dolomite samples in Bonifacie et al. (2017) cannot be recalculated with the new IUPAC parameters, thus it is not clear how much the calibration would change with the new parameters.

Due to the uncertainties in the dolomite-specific $Δ_{47}$ acid fractionation and its temperature-dependence and because dolomite reacts much faster at higher temperatures Bonifacie et al. (2017) published their calibration for an acid digestion temperature of 90 °C. In the ETH laboratory, dolomites and calcites are digested at 70 °C and at this temperature, a different-dolomite specific $Δ_{47}$ acid fractionation is observed (Müller et al., 2017a). In many new laboratories single bath preparation systems allowing the measurement of sub-milligram samples at 70 °C are becoming the method of choice for clumped isotope analysis. This is because the sample size reduction allows to carry out high-resolution paleo-climate reconstructions (Grauel et al., 2013; Rodríguez-Sanz et al., 2017; Breitenbach et al., 2018; Leutert et al., 2019) or the study of complex diagenetic vein fabrics (Millán et al., 2016; Smeraglia et al., 2018) that cannot be studied with conventional

common acid bath systems that require large samples. It is thus crucial to also produce a dolomite-specific $Δ_{47}$-temperature calibration at 70 °C and to evaluate potential differences with respect to the evaluation schemes using the calcite specific parameters. In addition, in this study we firmly anchor the results to the absolute reference frame using a calcite-based correction scheme using the widely distributed ETH Standards, which allows other laboratories to better compare the data to ours (Bernasconi et al., 2018). We produced a dolomite specific $Δ_{47}$ temperature calibration using natural and in laboratory synthesized (proto-)dolomite samples covering a temperature range from 25 to 1100 °C. We evaluated this new calibration and show results of potential dolomite standards and the advantages of their regular analysis for an improved inter-laboratory dolomite $Δ_{47}$ data comparison.

2. Materials and methods

2.1. Samples

To cover a wide temperature range we synthetized dolomites in the laboratory under controlled temperature conditions at 70, 140 and 220 °C. For low temperature we used samples of natural dolomites formed at 25 °C from Lagoa Vermelha (Brasil) the same lagoon from which Bonifacie et al. (2017) obtained their samples and at 32 °C in a sabkha environment in Qatar. Finally, we use two dolomites that were heated in a piston cylinder to 1100 °C to obtain a stochastic isotope composition. In total we analyzed 22 different samples between 6 and 87 times.

2.1.1. Dolomites synthesized in the laboratory at 70, 140 and 220 °C

Laboratory (proto-) dolomites were synthesized following the recipe described in Rodriguez-Blanco et al. (2015). Equimolar aqueous solutions of Na_2CO_3, $CaCl_2$ and $MgCl_2$ were mixed at room temperature, which led to an instantaneous precipitation of a white, gel-like solid confirmed by X-ray diffraction to be amorphous. This gel was heated at 70, 140 and 220 °C for between 1 day and 12 weeks. At selected time points, experimental runs were quenched to room temperature by taking them out of the oven into a cold water bath (it takes usually 5–10 min to reach room temperature), the solids separated from the supernatants via vacuum-filtration (0.2 μm polycarbonate Cyclopore filters, duration of vacuum-filtration is 1 min) and dried with

Table 1
Oxygen isotope fractionation between dolomite and fluid source and XRD parameters.

Identifier	T (°C)	Time (weeks)	$δ^{18}O_{VSMOW}$ (‰)	$δ^{18}O_{H2O,VSMOW}$ (‰)	$10^3 \ln α_{Dolomite-Water}$	d (104) (2θ)	Ordering ratio (015/110)	Mg%
LV 15 cm	25.5 ± 5.7		34.58 ± 0.05	1.8 ± 1.0	32.19	30.91	0.15	48.4
LV 71 cm	25.5 ± 5.7		34.39 ± 0.04	1.8 ± 1.0	32.01	30.83	0.22	45.9
Qatar 1	32 ± 6		35.11 ± 0.04			30.94	0.29	49.5
Leeds 23	70 ± 2	1.0	15.73 ± 0.05	−7.31 ± 0.1	22.95	30.78	0	44.4
Leeds 1	70 ± 2	1.1	15.97 ± 0.11	−7.35 ± 0.1	23.23	30.81	0	45.7
Leeds 6	70 ± 2	1.1	15.53 ± 0.06	−7.36 ± 0.1	22.79	30.84	0	46.3
Leeds 12	70 ± 2	2.4	15.53 ± 0.21	−7.28 ± 0.1	22.72	Na	Na	Na
Leeds 20	70 ± 2	4.0	15.59 ± 0.05	−7.33 ± 0.1	22.82	30.72	0.08	42.7
Leeds 81	70 ± 2	12.0	15.56 ± 0.10			30.89	0.08	48.0
Leeds 82	70 ± 2	12.0	15.98 ± 0.03	−5.99 ± 0.1	21.86	30.89	0	47.8
Leeds 83	70 ± 2	12.0	15.50 ± 0.10	−7.12 ± 0.1	22.53	30.80	0	44.9
Leeds 21	140 ± 2	1.0	7.85 ± 0.20	−7.31 ± 0.1	14.94	30.93	0	49.2
Leeds 14	140 ± 2	2.4	9.38 ± 0.09	−7.13 ± 0.1	16.49	30.90	0.21	48.0
Leeds 22	140 ± 2	4.0	9.30 ± 0.20	−7.10 ± 0.1	16.39	30.87	0.14	47.3
Leeds 15	140 ± 2	5.6	9.19 ± 0.07	−7.05 ± 0.1	16.22	30.90	0.21	48.1
Leeds 34	220 ± 2	2.1	6.14 ± 0.54	−6.91 ± 0.1	13.05	31.01	0.28	51.6
Leeds 41	220 ± 2	4.0	4.82 ± 0.44	−6.71 ± 0.1	11.54	31.00	0.32	51.3
Leeds 84	220 ± 2	12.0	4.92 ± 0.23	−4.74 ± 0.1	9.66	30.96	0.38	50.0
Leeds 85	220 ± 2	12.0	5.19 ± 0.21	−4.72 ± 0.1	9.91	30.96	0.39	50.0
Leeds 86	220 ± 2	12.0	5.74 ± 0.15	−5.37 ± 0.1	11.10	31.00	0.40	51.5

All uncertainties are displayed at the 95% CL; oxygen isotope composition of the fluid source of samples LV 15 cm and 71 cm are derived from van Lith et al. (2002); Mg% derived from equation $N_{CaCO_3} = 333.33*d(104) − 911.99$ with d value in Å of Lumsden and Chimahusky (1980).

isopropanol. The end products were determined to be (proto-)dolomite by X-ray diffraction. Ordered crystalline dolomite forms from an initial amorphous calcium-magnesium carbonate phase that first crystallizes to a non-stoichiometric proto-dolomite, and that then transforms over hours to weeks, depending on the temperature, to fully ordered stoichiometric dolomite (Rodriguez-Blanco et al., 2015). For our calibration we analyzed multiple samples at each of the three temperatures (8 at 70 °C, 4 at 140 °C and 5 at 220 °C, respectively, with experiment temperature uncertainty usually ± 2 °C; see Table 1). All laboratory samples do not react with 10% HCl, an indicator that was used already in the earliest studies (e.g. Dolomieu, 1791; Lumsden and Chimahusky, 1980) on dolomites to distinguish them from calcites or high magnesium calcites.

2.1.2. Microbial dolomite concretions from the Brazilian lagoon "Lagoa Vermelha"

For the low temperature range we included two dolomite concretions from a sediment core of Lagoa Vermelha (LV 15 cm, LV 71 cm). The lagoon is located about 100 km East of Rio de Janeiro, Brazil (Van Lith et al., 2002) and is a very shallow isolated lagoon influenced by recharge from the sea and mixing with meteoric water and evaporation which seasonally exceeds precipitation. This causes an annual wet-dry seasonal cycle with hypersaline conditions during the summer months. The dolomite concretions form during intense evaporative conditions, where the precipitation process is mediated by the increase of microbial activity and the presence of extracellular polymeric substances (EPS; Do Nascimento, 2018). The annual mean water temperature of Lagoa Vermelha is approximately 25 °C, and the recorded temperature in 20 cm sediment depth was 25.5 ± 5.7 °C from November 2011 till May 2015 (Do Nascimento, 2018) using an identical water temperature logger setup as Bahniuk et al. (2015) applied for the nearby lagoon Brejo do Espinho. The XRD analyses on these two natural samples were done on finely grinded powders without any washing or purification treatment. For Δ_{47} analyses we first analyzed a number of replicates of untreated samples, before measuring more replicates of the same samples after purification with 10% hydrogen peroxide to remove organic matter followed by rinsing several times with deionized water. In this way we treated the dolomite the same way as Bonifacie et al. (2017), which also included samples from Lagoa Vermelha in their calibration.

2.1.3. Dolomite from Qatar

The dolomite sample is from the Dohat Faishakh sabkha, Qatar, which is located on the western coast of the Qatar peninsula (Brauchli et al., 2016; Illing et al., 1965). It was extracted from a short core collected in the supratidal zone at 40 cm depth, where dolomite is the only carbonate mineral present. This dolomite was interpreted to be a primary precipitate from the pore fluids and not a replacement of calcite or aragonite (Brauchli et al., 2016). Unfortunately there are no long term temperature measurements at this location. At the time the sample for this study was collected during the month of March, the sediment temperature was 29 °C. Within the sediments of the supratidal zone of the same sabkha "a few inches below the surface", Illing et al. (1965) measured temperatures of 33 to 34 °C in November. In a detailed study of the Trucial coast sabkha (Abu Dhabi), which is very similar to the Dohat Faishakh sabkha in terms of general environment and climate, Butler (1969) concluded that a depth of 50 cm the annual temperature range is 23 to 41 °C with an average of 32 °C. Thus we assign a temperature of 32 ± 6 °C to this sample.

2.1.4. Dolomites heated to 1100 °C in a piston cylinder

Fine powder of two natural dolomites (from Monte San Salvatore, Switzerland and La Roda, Spain) was heated during 4 h at 1100 °C in a piston cylinder apparatus. More detail on these dolomite samples with stochastic isotope distribution are in (Müller et al., 2017a) where these samples, labelled as Sansa (H) and Rodolo (H), were used to determine

the absolute Δ_{47} AFF. In this study these are the hottest calibration samples. General estimates for calcite or dolomite Δ_{47} blocking temperatures during cooling range between 200 and 300 °C, respectively (e.g. Bonifacie et al., 2017; Ryb et al., 2017). However, from the observations of the heating study in Müller et al. (2017a) where calcites were scrambled at 1000 °C in two different heating devices and retained the same Δ_{47} signature although cooling of a piston cylinder is achieved in less than 1 min and for a Patterson rig apparatus it takes about 45 min, we do not expect that solid state reordering during cooling had any impact on these high temperature Δ_{47} signatures. These samples are important for a more accurate interpretation of natural dolomites that retained extremely hot temperature signals near magmatic intrusions (e.g. Lloyd et al., 2017; Ryb et al., 2017; Lloyd et al., 2018).

2.2. Natural dolomites from Monte San Salvatore, Switzerland, La Roda, Spain and the international standard NIST SRM 88b

The dolomite from Monte San Salvatore, Southern Switzerland, is a replacement dolomite that formed during the middle Triassic (Lehner, 1952; Zorn, 1971) and was collected along the road leading southwards from Lugano at the locality Forca di San Martino. We named the sample "Sansa" to avoid confusion with the dolomites from San Salvador Island discussed by Murray and Swart (2017).

The other natural sample comes from La Roda, Spain and is a lacustrine poorly-ordered dolomite that formed during the Pliocene probably induced by microbial activity (García del Cura et al., 2001). Additionally we analyzed the NIST (National Institute of Standards and Technology, Gaithesburg, MD, USA) dolomite standard SRM 88b, which is a natural dolomite from the Silurian Racine formation, northeastern Illinois. This widely available dolomite standard was already measured in other clumped isotope studies (e.g. Defliese et al., 2015; Murray et al., 2016) and enables a direct comparison between different laboratories.

2.3. X-ray diffraction and stable isotope analyses

All samples were drilled from the hand specimens with a hand-held dental drill taking care of not overheating the drill bit to avoid potential isotopic reordering. The mineralogy and degree of ordering was determined with a Powder X-ray Diffractometer Bruker AXS D8 Advance equipped with a Lynxeye detector. Oxygen, carbon and clumped isotope compositions were determined with a Kiel IV carbonate device coupled to a MAT 253 isotope ratio mass spectrometer (Thermo Fisher Scientific) as thoroughly described in earlier studies (Schmid and Bernasconi, 2010; Meckler et al., 2014; Müller et al., 2017b). Briefly, 130 to 160 μg of calcite standards (ETH-1 to -4) and samples were weighed in glass vials and placed in the Kiel IV carbonate device (46 samples per measurement sequence). The samples are reacted at 70 °C with three drops of 104% phosphoric acid and during the reaction with the acid (300 s for calcite and 1200 s for dolomite) the released CO_2 gas is constantly frozen in the liquid nitrogen (LN_2) trap 1 of the Kiel device. For the measurement sequences of this dolomite study, the ETH calcite standards were treated identically to the unknown (proto-)dolomite samples with 1200 s reaction time. As the produced CO_2 gas is continuously frozen away during the phosphoric acid reaction in the Kiel IV carbonate device, the longer reaction time does not increase the time of CO_2 gas being in contact with evolved H_2O molecules from the acid reaction and no effect of the acid reaction length on the measured raw Δ_{47} values of the calcite standards was observed. After the reaction is completed trap 1 is heated to −100 °C and the gas is transferred through a tubing filled with 10 mm Porapak Type Q (50–80 mesh) embedded in silver wool into a second LN_2 trap. The Porapak trap was kept between −20 and −14 °C to remove potential contaminants such as halo-/hydrocarbons or reduced sulfur compounds. The samples were measured in the LIDI mode that measures the sample gas once for 600 s and subsequently the working gas during 600 s. Usually the

measurements start at 20 to 25 V on mass 44 and decrease by approx. 10 V during the 600 s (Hu et al., 2014; Müller et al., 2017b). Before starting a measurement sequence peak shape scans in the range of 30 to 10 V on m/z 44 are carried out at different gas pressures to determine the pressure dependence of the negative backgrounds to do a so-called pressure-sensitive baseline correction (PBL correction) according to (Bernasconi et al., 2013; Meckler et al., 2014; Müller et al., 2017a). The raw data are processed with the free Easotope software (John and Bowen, 2016), by first doing the PBL correction, then it calculates the carbon and oxygen isotope composition of the carbonates in the delta notation relative to the international Vienna PeeDee Belemnite standard, VPDB ($\delta^{13}C_{VPDB}$, $\delta^{18}O_{VPDB}$ in ‰) using the parameters recommended by Daëron et al. (2016). The calculated PBL-corrected clumped isotope composition (Δ_{47raw}) relative to our working gas ($\delta^{13}C_{VPDB}$ = −7.25 ‰, $\delta^{18}O_{VPDB}$ = +1.65 ‰) for each replicate was converted to $\Delta_{47\ CDES\ 70°C}$ (‰) with an empirical transfer function (ETF) constructed from the accepted vs. measured Δ_{47} values of a moving window of 32 standards (ETH-1,-2,-3,-4's) before and after the unknown sample (see Bernasconi et al., 2018). The results are presented as the averages of replicates measured over a long period of time, from 2015 to 2017, where the conditions of the analytical instruments changed several times. Our measurement strategy involves the measurement of only few replicates of the same sample in the same measurement sequence of 46 samples. The distribution of replicates over multiple runs during different correction intervals often comes with the cost of a worse precision compared to measuring many replicates of the same sample in one analytical sequence or a short time interval, but we expect that this leads to more accurate Δ_{47} estimates as it removes possible day to day biases. For the conversion into the absolute reference frame Easotope uses the accepted Δ_{47} values of the calcite standards ETH-1 to -4 as reported in Bernasconi et al. (2018) that were prior determined with heated and equilibrated gases according to Dennis et al. (2011) in Meckler et al. (2014). Here we report the results for a reaction temperature of 70 °C ($\Delta_{47\ CDES\ 70°C}$) and refrain to project them to an acid digestion temperature of 25 °C due to the large uncertainties in the AFF of dolomite (see different observations in Defliese et al., 2015; Murray et al., 2016; Müller et al., 2017a). For $\delta^{18}O$ we used an AFF of 1.009926 for dolomite (Rosenbaum and Sheppard, 1986). Conversion from VPDB to the VSMOW scale was done using $\delta^{18}O_{SMOW}$ = 1.03091 * $\delta^{18}O_{PDB}$ + 30.91 (Coplen et al., 1983). The

oxygen and carbon isotopes of the samples were corrected using the accepted ETH calcite standard values that were determined relative to international standards NBS 18, NBS 19 and LSVEC in three different laboratories (see Bernasconi et al., 2018). The Δ_{47} temperatures of the ETH calcite calibration were the fully recalculated calcite Δ_{47}-T calibration of Kele et al. (2015) for 70 °C acid digestion temperature using the isotopic parameters recommended in Daëron et al. (2016) including the fully recalculated accepted ETH standard values from Bernasconi et al. (2018) without projecting them to a 25 °C acid digestion temperature with the correction factor of 0.062 ‰ (ETH-1: Δ_{47} = 0.196 ‰, ETH-2: Δ_{47} = 0.194 ‰, ETH-3: Δ_{47} = 0.629 ‰ and ETH-4: Δ_{47} = 0.445 ‰).

Oxygen isotopes in waters from the experiments were measured with the CO_2 equilibration method. 200 μl of water are pipetted in 12 ml septum-capped vials which are subsequently filled with a mixture of 0.3 % CO_2 and He. After equilibration at 25 °C for at least 18 h the CO_2/He mixture is measured using a Thermo Scientific Gas Bench II connected to a Thermo Scientific Delta V plus isotope ratio mass spectrometer. The system is calibrated with the international standards SMOW, SLAP and GISP. The results are reported in the conventional delta notation with respect to VSMOW (Coplen, 1996). Reproducibility of the measurements based on repeated measurements of an internal standard was better than 0.06 ‰.

3. Results

3.1. (Proto-)dolomite mineralogy

The natural dolomites from Lagoa Vermelha, Brazil all show the main dolomite reflections 104, 110 and 113 at the corresponding 2θ space and the dolomite ordering reflections 015 and 021 (Bradley et al., 1953; Goldsmith and Graf, 1958; Gregg et al., 2015). Whereas the ordering reflection 101 is lacking in the XRD pattern of LV 15 cm. In LV 71 cm there could be a small reflection but it is masked by a large reflection from an unidentified phase (Fig. 1). In both samples the ordering reflection 015 is clearly smaller than the 110 reflection, with an ordering ratio (015)/(110) of 0.15 and 0.22 for LV 15 cm and LV 71 cm, respectively. The Mg content was determined from the position of the main dolomite reflection d(104) and the relationship for the molar Ca content in a pure $Mg,Ca(CO_3)_2$ (N_{CaCO3} = 333.33*d(104)-911.99 with d
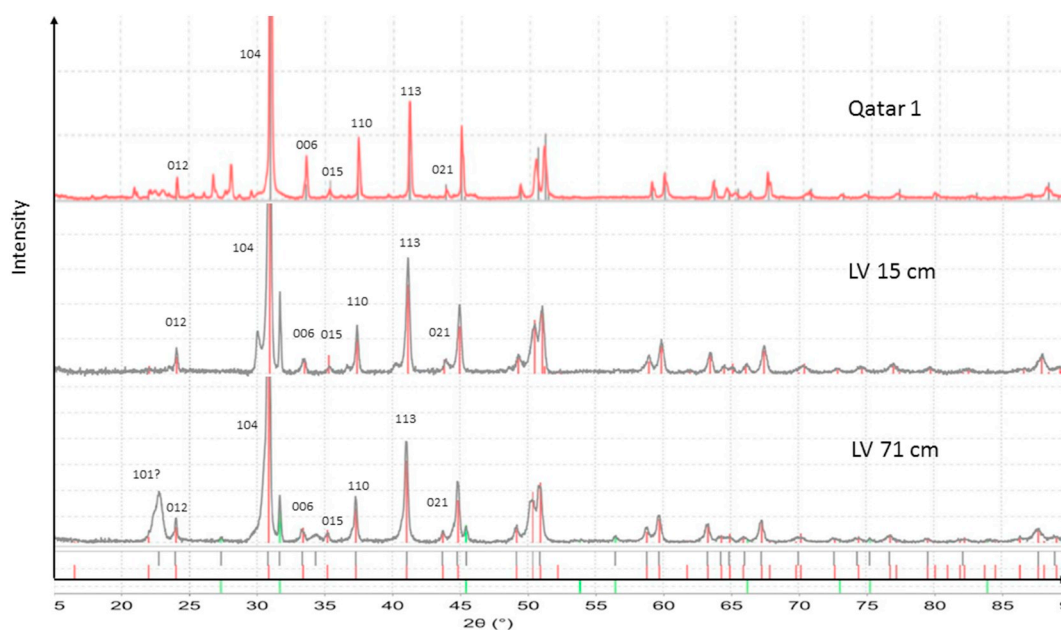

Fig. 1. X-ray diffraction pattern of the two natural calibration samples retrieved from the sediments of the Brazilian Lagoa Vermelha and the one of Qatar. The sample names are indicated in the right area for each of the three XRD patterns.

value in Å) derived in Lumsden and Chimahusky (1980) and varies between 45.9 and 48.4% (Table 1). In sample LV 71 cm the presence of halite (NaCl; as we did the XRD analysis at powdered samples that were not H_2O_2 treated) is visible indicated by the green reflections at 32 and around 45°, whereas for sample LV 15 cm it is not as clear as the reflection around 45° is not visible. With almost all dolomite ordering reflections expressed, the carbonate phase of LV 15 cm and LV 71 cm can be described as poorly ordered dolomite. The natural sample from Qatar has a Mg content of 49.5 %, all ordering peaks, besides the 101 reflection, are clearly visible and the (015)/(110) ratio is with 0.29 slightly better expressed than the other two natural samples from Brazil (see Fig. 1 and Table 1).

The XRD patterns of the 'dolomite samples' synthesized in the laboratory (Table 1 and Fig. 2) at 70 °C did not show the 'ordered' 101, 015 and 021 dolomite reflections (only samples Leeds 20 and 81 show a small reflection at the position of 015), pointing to a crystal structure typical for proto-dolomite (see Graf and Goldsmith, 1956) which is called by some authors very high Mg-calcite (VHMC) (Gregg et al., 2015). This observation was independent of the length of equilibration at the experiment temperature of 70 °C (1 to 12 weeks). In our study we name the 70 °C samples proto-dolomite as from their Mg contents between 42.7 and 48.4 % and their property not to react with 10% HCl they are more similar to ideal crystalline dolomite than a high Mg calcite phase. Thereof the Mg content is not increasing with increasing experimental time and no trend is observed. Samples crystallized at 140 °C exhibited in their XRD pattern the ordering reflections of dolomite 015 and 021, but still lacked the 101 reflection pointing to poorly ordered dolomite with (015)/(110) ratios between 0.14 and 0.21 and Mg content close to stoichiometric dolomite of 47.3 to 49.2 %. The XRD pattern of Leeds 21, with only 1 week the shortest analyzed 140 °C sample, shows no 015 ordering reflection, but seems to be stoichiometric proto-dolomite. Finally, the XRD patterns of the samples synthesized at 220 °C clearly display all three dolomite ordering reflections and all of the analyzed samples are stoichiometric. The 015 ordering reflection is much more expressed than for the samples synthesized at lower temperatures and the degree of ordering is increasing from 0.28 for the 2.1 week experiment (Leeds 34) up to around 0.4 for the 12 weeks experiments (Leeds 84–86 in Table 1). Comparison to the study of Gregg et al. (2015) this would be not ideally ordered dolomite,

but we would not call it a poorly ordered dolomite anymore as for the 140 °C samples (see lower XRD pattern in Fig. 2). Although the proto-dolomite samples synthesized at 70 °C show no 015 ordering reflection and their Mg content varied between 42 and 48 %, their dissolution rate when exposed to 10% HCl or 104% phosphoric acid was much slower than what we observe for a typical calcite or high Mg-calcite (15 mol % Mg), an observation commonly used in older studies to distinguish dolomite from calcites (e.g. Dolomieu, 1791; Lumsden and Chimahusky, 1980).

The dolomites NIST SRM 88b and Sansa are well-ordered and stoichiometric dolomites (see Table 3). All ordered dolomite reflections are visible and the 015 reflections are almost as intense as the 110 (Fig. 3) similar to the "near perfect ordering" example Bonneterre dolomite described in Gregg et al. (2015). The Rodolo dolomite is stoichiometric, but the ordering reflections are moderately well expressed with (015)/(110) of 0.35. The Rodolo dolomite is thought to be a direct precipitate from solution in a lacustrine environment (García del Cura et al., 2001), in contrast to the other diagenetic dolomites that are a replacement of calcite or aragonite.

3.2. Dolomite-water oxygen isotope fractionation

The averages of the measurements of all samples used for the dolomite Δ_{47}-T calibration are displayed in Tables 1 and 2 and the results of individual measurements are reported in Table S1. For the natural samples the fractionation ranges tightly between 32.01 and 32.19 ‰. The oxygen isotope composition of the water of Lagoa Vermelha is not exactly known and the value taken from van Lith et al. (2002) of 1.8 ‰ has an assigned larger uncertainty because of the annual variations in hydrology of the lagoon.

For the synthetic dolomites that were equilibrated with the solutions for variable times ranging from 1 to 12 weeks, we obtained a larger spread in the results (70 °C samples: 21.86–23.23 ‰; 140 °C samples: 14.94–16.49 ‰; 220 °C samples: 9.66–13.05 ‰), thereof especially the shortest 140 °C experiment Leeds 21 (the only sample of this temperature that still displays a proto-dolomite XRD pattern) shows a lighter $\delta^{18}O$. Further on the water value of sample 82 seems to be affected by evaporation during water sample transport prior to isotope analysis as all the other values vary in a narrow range and the only
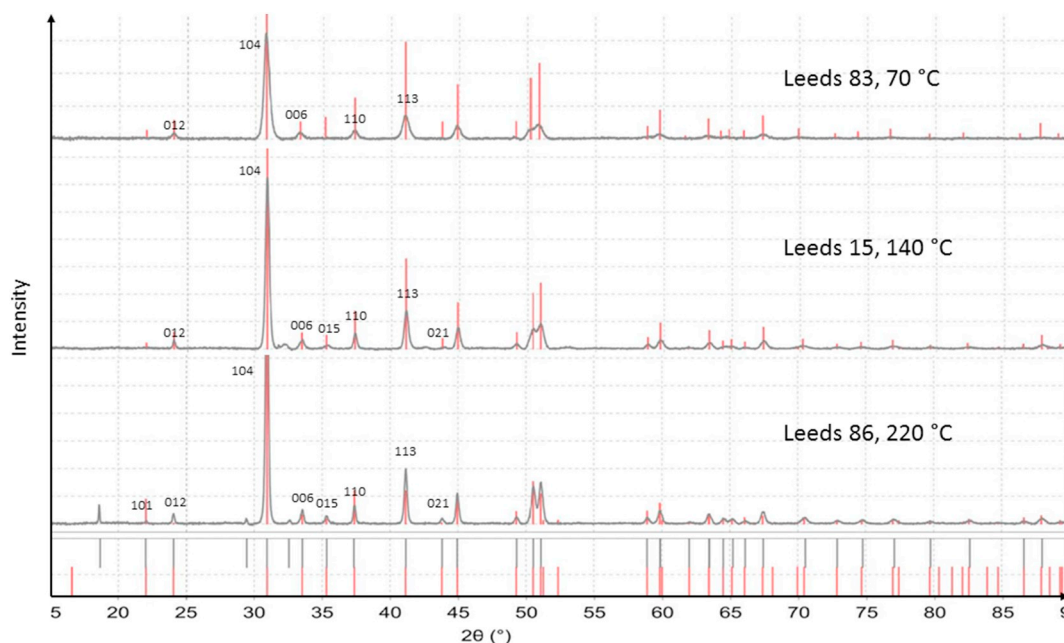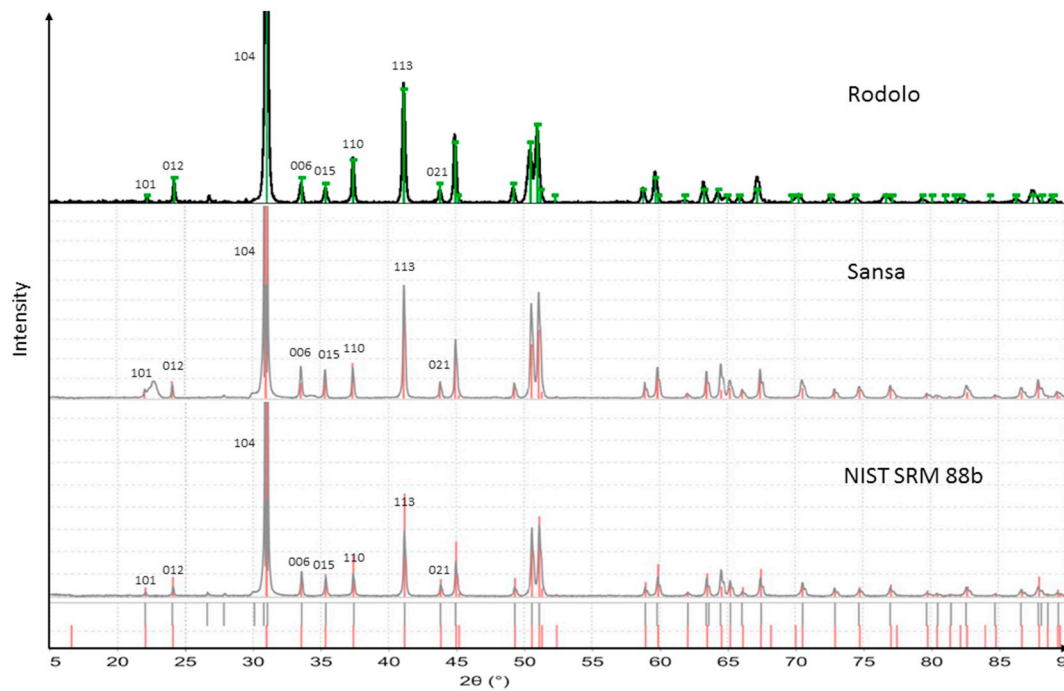

Fig. 2. The typical XRD patterns of 'dolomite' samples synthesized under controlled laboratory conditions (Table 1); upper pattern 70 °C, 12 weeks; middle pattern 140 °C, 5.6 weeks; and lower pattern 220 °C, 12 weeks.

Fig. 3. XRD pattern of the poorly-ordered stoichiometric lacustrine dolomite Rodolo (upper green XRD pattern) and the two ideally ordered stoichiometric dolomites Sansa (middle XRD pattern) and the international standard NIST SRM 88b (lower XRD pattern). (For interpretation of the references to colour in this figure legend, the reader is referred to the web version of this article.)

2.1 weeks short 220 °C experiment Leeds 34 showed the largest fractionation to the experimental solution. However, there is not clear observable trend in the isotopes that correlates with the increasing degree of ordering. The uncertainty of the oxygen isotope composition of the (proto-)dolomite samples varies between ± 0.03–0.44 ‰ at the 95% Cl, which takes into account the number of replicates per sample (indicated in last column of Table 2).

Table 2 shows the average $\delta^{13}C_{VPDB}$ and $\delta^{18}O_{VPDB}$, the bulk isotope composition relative to our reference gas (δ^{47}) and the clumped isotope composition for an acid digestion temperature of 70 °C ($\Delta_{47\ CDES\ 70°C}$) of all samples. All uncertainties are reported at the 95% Cl and range between 0.02 and 0.14 ‰ for $\delta^{13}C_{VPDB}$, 0.04–0.54 ‰ for $\delta^{18}O_{VPDB}$,

0.05–0.77 ‰ for δ^{47} and 0.010–0.054 ‰ for $\Delta_{47\ CDES\ 70°C}$.

The average $\Delta_{47\ CDES\ 70°C}$ values of the two "cold" natural dolomite calibration samples are 0.637 ‰ for LV 15 cm and 0.619 ‰ for LV 71 cm, both samples have similar oxygen isotope composition, but their carbon isotope compositions are more distinct with −8.32 ‰ for the more shallow sample and −10.21‰ for the deeper one. We did not observe any significant differences between replicates untreated and treated with 10% H_2O_2 (see individual replicates displayed in Table S1) and therefore do not consider them separately. The $\delta^{13}C_{VPDB}$ and $\delta^{18}O_{VPDB}$ of the synthetic samples are quite similar to each other and the $\Delta_{47\ CDES\ 70°C}$ values range between 0.497 and 0.515 ‰ for samples synthesized at 70 °C, between 0.398 and 0.426 ‰ for samples

Table 2
Averages of (proto-)dolomite Δ_{47}-T calibration samples.

Identifier	T (°C)	$\delta^{13}C_{VPDB}$ (‰)	$\delta^{18}O_{VPDB}$ (‰)	δ^{47} (‰)	$\Delta_{47\ CDES\ 70°C}$ (‰)	#
LV 15 cm	25.5 ± 5.7	−8.32 ± 0.02	3.56 ± 0.05	10.87 ± 0.08	0.637 ± 0.022	16
LV 71 cm	25.5 ± 5.7	−10.21 ± 0.02	3.38 ± 0.04	8.83 ± 0.07	0.619 ± 0.019	16
Qatar 1	32 ± 6	5.02 ± 0.01	4.06 ± 0.03	24.67 ± 0.05	0.611 ± 0.015	25
Leeds 23	70 ± 2	−7.07 ± 0.03	−14.72 ± 0.05	−6.81 ± 0.12	0.508 ± 0.017	16
Leeds 1	70 ± 2	−7.10 ± 0.04	−14.51 ± 0.11	−6.70 ± 0.11	0.497 ± 0.014	12
Leeds 6	70 ± 2	−7.17 ± 0.03	−14.90 ± 0.06	−7.07 ± 0.06	0.523 ± 0.020	11
Leeds 12	70 ± 2	−7.12 ± 0.09	−14.92 ± 0.21	−7.10 ± 0.26	0.504 ± 0.037	8
Leeds 20	70 ± 2	−7.22 ± 0.02	−14.86 ± 0.05	−7.13 ± 0.08	0.515 ± 0.042	9
Leeds 81	70 ± 2	−7.24 ± 0.04	−14.89 ± 0.10	−7.09 ± 0.10	0.515 ± 0.022	18
Leeds 82	70 ± 2	−7.12 ± 0.02	−14.48 ± 0.03	−6.67 ± 0.07	0.499 ± 0.016	21
Leeds 83	70 ± 2	−7.25 ± 0.04	−14.94 ± 0.10	−7.15 ± 0.11	0.513 ± 0.015	41
Leeds 21	140 ± 2	−7.38 ± 0.02	−22.37 ± 0.20	−15.09 ± 0.19	0.426 ± 0.027	6
Leeds 14	140 ± 2	−7.30 ± 0.03	−20.88 ± 0.09	−13.61 ± 0.18	0.398 ± 0.014	15
Leeds 22	140 ± 2	−7.35 ± 0.06	−20.96 ± 0.20	−13.74 ± 0.30	0.401 ± 0.015	9
Leeds 15	140 ± 2	−7.32 ± 0.04	−21.07 ± 0.07	−13.75 ± 0.15	0.409 ± 0.021	21
Leeds 34	220 ± 2	−7.45 ± 0.14	−24.03 ± 0.54	−16.95 ± 0.70	0.322 ± 0.054	6
Leeds 41	220 ± 2	−7.45 ± 0.07	−25.31 ± 0.44	−18.43 ± 0.77	0.348 ± 0.025	6
Leeds 84	220 ± 2	−7.42 ± 0.02	−25.21 ± 0.23	−18.25 ± 0.37	0.311 ± 0.018	12
Leeds 85	220 ± 2	−7.42 ± 0.02	−24.95 ± 0.21	−17.91 ± 0.30	0.316 ± 0.028	16
Leeds 86	220 ± 2	−7.31 ± 0.02	−24.42 ± 0.15	−17.31 ± 0.24	0.320 ± 0.017	11
Rodolo (H)	1100	−3.89 ± 0.02	1.78 ± 0.04	13.16 ± 0.05	0.230 ± 0.010	87
Sansa (H)	1100	1.29 ± 0.02	−3.68 ± 0.04	12.54 ± 0.06	0.228 ± 0.011	59

All uncertainties are displayed at the 95% CL.

synthesized at 140 °C and between 0.311 and 0.348 ‰ for the 220 °C samples (the Δ_{47} value of sample Leeds 34 matches well the other 220 °C samples and shows no sign of dis-equilibrium). There is only the shortest 140 °C experiment Leeds 21 (the only proto-dolomite of the 140 °C samples) that shows a Δ_{47} slightly bigger than the other samples synthesized at same temperature. However, this could be an effect of the poor measurement replication as discussed in Fernandez et al. (2017) as this sample was only analyzed 6 times. The two natural dolomites that where heated to 1100 °C to produce a stochastic isotope distribution were replicated much more and show almost identical Δ_{47} $_{CDES\ 70°C}$ values with 0.230 ± 0.010 ‰ for Rodolo (H) and 0.228 ± 0.011 ‰ for Sansa (H).

Using only the (proto-)dolomites synthesized under controlled laboratory conditions without the two heated dolomites and the three natural dolomites from the Brazilian lagoon and from Qatar, we obtain a temperature dependence with $R^2 = 0.9862$ for the oxygen isotope fractionation relative to water of

$$10^3\alpha_{Dolomite-Water} = 2.7757 \pm 0.2062 \times \left(\frac{10^6}{T^2}\right) - 0.6314 \pm 1.3916$$

For this temperature dependence we did not use sample Leeds 82 and sample Leeds 34 due to the aforementioned points. The natural samples of Lagoa Vermelha were not included due to the higher uncertainty in the $\delta^{18}O$ of the fluid source.

3.3. Clumped isotope fractionation

We observed some scatter in the conventional isotopes, but we did not observe trends correlating with differences in the mineralogy and the Δ_{47}. Only the shortest experiment at 140 °C is slightly heavier than the longer 140 °C experiments that could be due to dis-equilibrium with the 140 °C environment as indicated by the absence of the 015 ordering reflection, or it is due to the small number of replicates. All the other Δ_{47} compositions for the samples of a certain temperature match nicely. There is no trend over the course of the experiments to observe and it seems the rest of the samples records the designated temperatures.

The clumped isotope composition of individual replicates and averages of samples formed between 25 and 220 °C is plotted in Fig. 4

against their reciprocal formation temperatures ($10^6/T^2$). From all analyzed individual replicates we obtained a linear regression (calculated with the Linear Regression function in excel without taking into account the minor effects of T uncertainties derived of the three cold natural samples) for the $\Delta_{47\ CDES\ 70°C}$ – T relationship with $R^2 = 0.864$ of

$$\Delta_{47\ CDES\ 70°C} = 0.0428 \pm 0.0020 \times \left(\frac{10^6}{T^2}\right) + 0.1481 \pm 0.0160$$

that is valid for acid digestion of (proto-)dolomites at 70 °C and with the temperature in Kelvin. The narrow 95% confidence interval envelope shows the well constrained linear regression that is based on 289 individual measurements of 20 different samples formed at 5 different temperatures. The averages of the Δ_{47} values of the 20 samples are displayed with their uncertainty at the 95% confidence level and for the reciprocal temperature uncertainty it correspond to the standard deviation of temperature estimates for each sample. The wider 95% prediction interval in Fig. 4 would correspond to the range any further individual analysis would fall to 95% probability. Due to the high number of measurements included in this calibration, of many samples spread over a much wider temperature range than existing studies (analogues to the calibrations of Kele et al., 2015 (recalculated in Bernasconi et al., 2018); Kluge et al., 2015; Winkelstern et al., 2016 (recalculated in Petersen et al., 2019); Bonifacie et al., 2017), the uncertainty of the linear relationship is very small (see Zaarur et al., 2013; Fernandez et al., 2017). Including the two measurements of the two dolomites that were heated and equilibrated during 4 h at 1100 °C (Müller et al., 2017a) the best fit is obtained when using a polynomial function of third order with $R^2 = 0.924$

$$\Delta_{47\ CDES\ 70°C}(‰) = -0.0002 \times \left(\frac{10^6}{T^2}\right)^3 + 0.0041 \times \left(\frac{10^6}{T^2}\right)^2 + 0.0115 \times \left(\frac{10^6}{T^2}\right) + 0.2218$$

based on a total of 435 individual sample measurements (Fig. 5). and about 1500 individual standard measurements (ETH-1,-2,-3,-4s) used for the data processing of these samples.

3.4. Stable isotope data of proposed dolomite reference materials

The isotopic compositions of the poorly ordered Rodolo dolomite
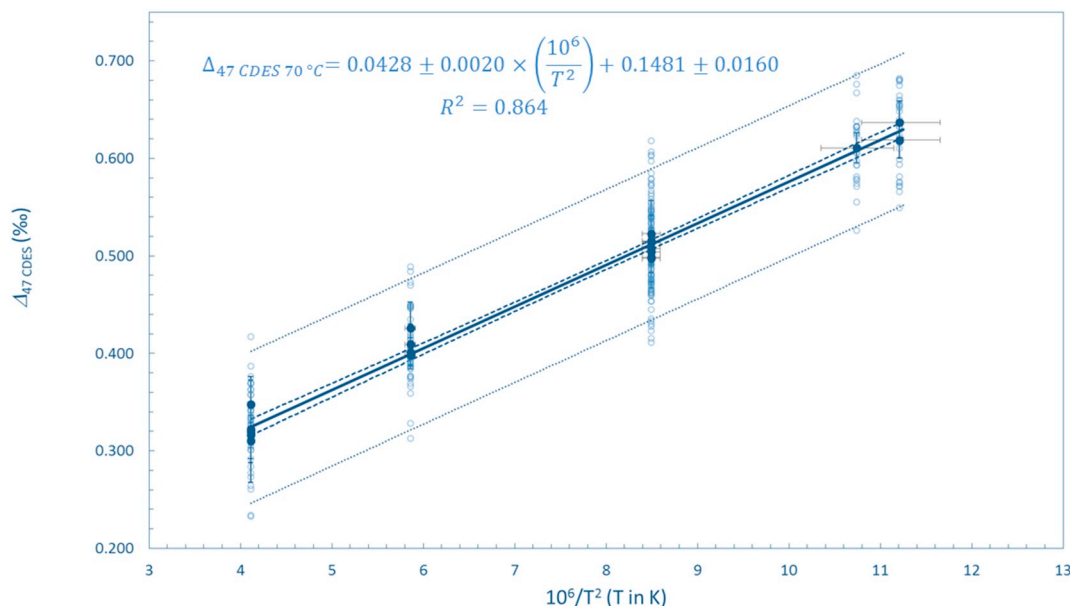
Fig. 4. The clumped isotope composition of the synthetic and natural (proto-)dolomite calibration samples digested at 70 °C is plotted against the reciprocal formation temperature. The linear relationship displayed in the top left is derived from the 289 individual replicates of the samples formed at temperatures between 25 and 220 °C. Averages of the 20 different samples are displayed as diamonds with their Δ_{47} uncertainty at the 95% Cl and the T uncertainty at the SD. The narrow dashed envelope corresponds to the 95% confidence interval of the calibration and the wider dotted envelope corresponds to the 95% prediction interval.
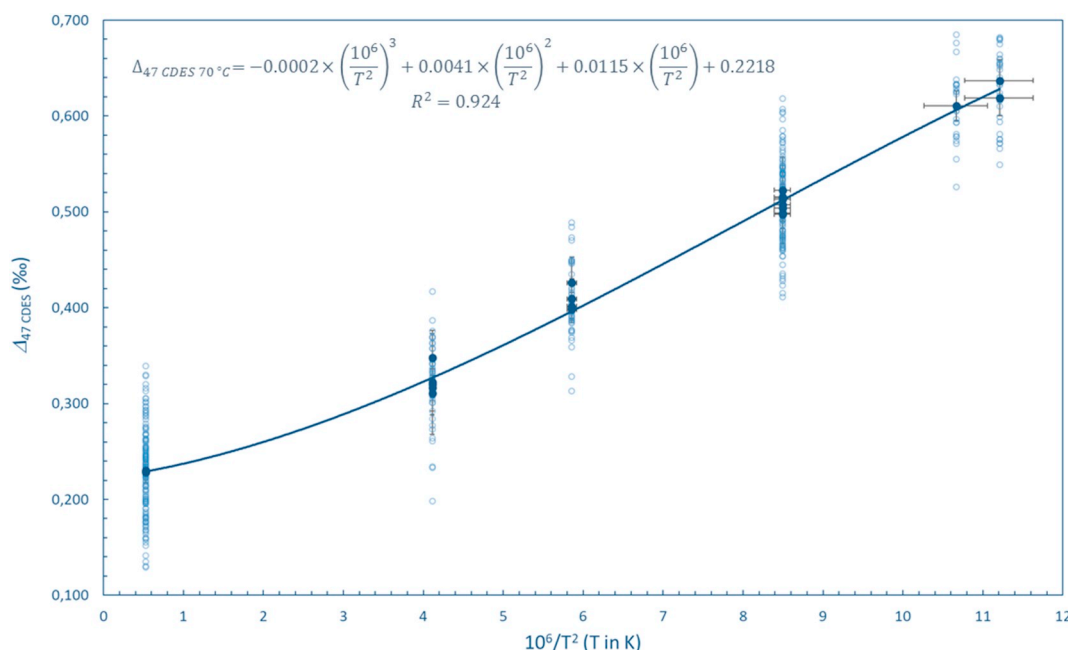
Fig. 5. Including the two dolomite samples that were heated to 1100 °C we obtain a third order polynomial Δ_{47}-T relationship based on 435 individual measurements covering the full range of potential formation temperatures of dolomite rocks.

and the two well-ordered dolomites are summarized in Table 3 (with uncertainties in the table at the 95% CI, but here in the text at the standard deviation of the mean) and with the individual replicates in the supplementary Table S2. The poorly ordered lacustrine Rodolo dolomite has a $\delta^{13}C_{VPDB}$ of -3.71 ± 0.06 ‰ and a relatively high $\delta^{18}O_{VPDB}$ of 2.77 $\pm$ 0.12 ‰ with the uncertainty displayed at the long-term standard deviation we obtained for 151 replicates measured over 2 years. Because of the large number of replicates the Δ_{47} of 0.632 ‰ is well constrained with an uncertainty of only $\pm$ 0.006 ‰ at the 95% CI giving a temperature of 25 $\pm$ 2 °C and a fluid source with $\delta^{18}O$ of +1.7 $\pm$ 0.04 ‰. The other two diagenetic dolomites which were not measured as many times and within less than a year, have almost identical Δ_{47} with 0.526 $\pm$ 0.014 ‰ for Sansa and 0.522 $\pm$ 0.022 ‰ for NIST SRM 88b. Whereas their $\delta^{13}C$ are similar (1.45 $\pm$ 0.09 ‰ and 2.12 $\pm$ 0.10 ‰), their oxygen isotope composition is different with -3.56 ± 0.18 ‰ for Sansa and -7.09 ± 0.13 ‰ for NIST SRM 88b. The two diagenetic dolomites are more difficult to react with phosphoric acid compared to the Rodolo, which is the cause of the worse reproducibility amongst all individual replicates measured during one year (Table S2), however, the Δ_{47} values reproduce extremely well.

4. Discussion

4.1. (Proto-)dolomite specific Δ_{47}-temperature calibration

4.1.1. Clumped isotope temperature relationship for 70 °C acid digestion
We start by comparing our new (proto-)dolomite calibration with the calcite calibration produced at ETH with the same instrumentation

and normalized to the CDES using the same ETH-1,-2,-3,-4 calcite standards, thus we can exclude methodological artefacts and data processing differences (IUPAC parameters). We note that for this study we reacted both calcites and dolomites for 20 min with continuous freezing of the CO_2 gas with liquid nitrogen during the entire reaction to comply with the principle of equal treatment of sample and standards. Comparison with the calcite calibration of Kele et al. (2015) recalculated in Bernasconi et al. (2018) shows a slightly shallower slope within the uncertainties of each other (0.0428 $\pm$ 0.0020 vs. 0.0449 $\pm$ 0.0019). However, the intercept of the calcite calibration is significantly lower so that the two calibrations do not overlap at their 95% CI's (Fig. 6). Statistical evaluation of our two laboratory-internal calibrations was done with the statistical software GraphPad Prism 7.01 and revealed that the difference in the slopes is not significant ($P = 0.1726$), but then after pooling data to a common slope reveals a significant difference between their y-intercepts ($P < 0.0001$; after Zar, 1984; see weblink https://www.graphpad.com/guides/prism/7/curve-fitting/index.htm?Reg_Comparingslopesandintercepts.htm). The use of the calcite calibration for dolomites formed at temperatures between 0 and 100 °C and acid digested at 70 °C would lead to calculated formation temperatures lower by 3 to 16 °C compared to the dolomite-specific calibration. Thus we conclude that calcite and dolomite have to be treated separately when measured for clumped isotopes, especially when reacted with phosphoric acid temperatures below 90 °C due to the different phosphoric acid fractionation factor.

In the past, clumped isotope analyses on natural dolomites were mostly treated the same way as calcites due to the fact that no dolomite specific Δ_{47} temperature calibrations and no dolomite specific AFF were

Table 3
Dolomite standards.

Identifier	$\delta^{13}C_{VPDB}$ (‰)	$\delta^{18}O_{VPDB}$ (‰)	$\Delta_{47\ CDES,\ 70°C}$ (‰)	T (°C)	$\delta^{18}O_{fluid}$ (‰)	#	d (104) (2θ)	Ordering ratio (015/110)	Mg%
Rodolo	-3.71 ± 0.01	2.77 $\pm$ 0.02	0.632 $\pm$ 0.006	25 $\pm$ 2	1.7 $\pm$ 0.4	151	30.95	0.35	50.0
Sansa	1.45 $\pm$ 0.04	-3.56 ± 0.09	0.526 $\pm$ 0.014	64 $\pm$ 6	2.8 $\pm$ 1.0	19	30.98	0.91	50.7
NIST SRM 88b	2.12 $\pm$ 0.06	-7.09 ± 0.08	0.522 $\pm$ 0.022	66 $\pm$ 10	-0.5 ± 1.5	14	30.99	0.92	50.7

All uncertainties are displayed at the 95% CI, $\delta^{18}O_{fluid}$ calculated by using combined T relationship of this study; Mg% derived from equation $N_{CaCO3} = 333.33*d$ (104) − 911.99 with d value in Å of Lumsden and Chimahusky (1980).
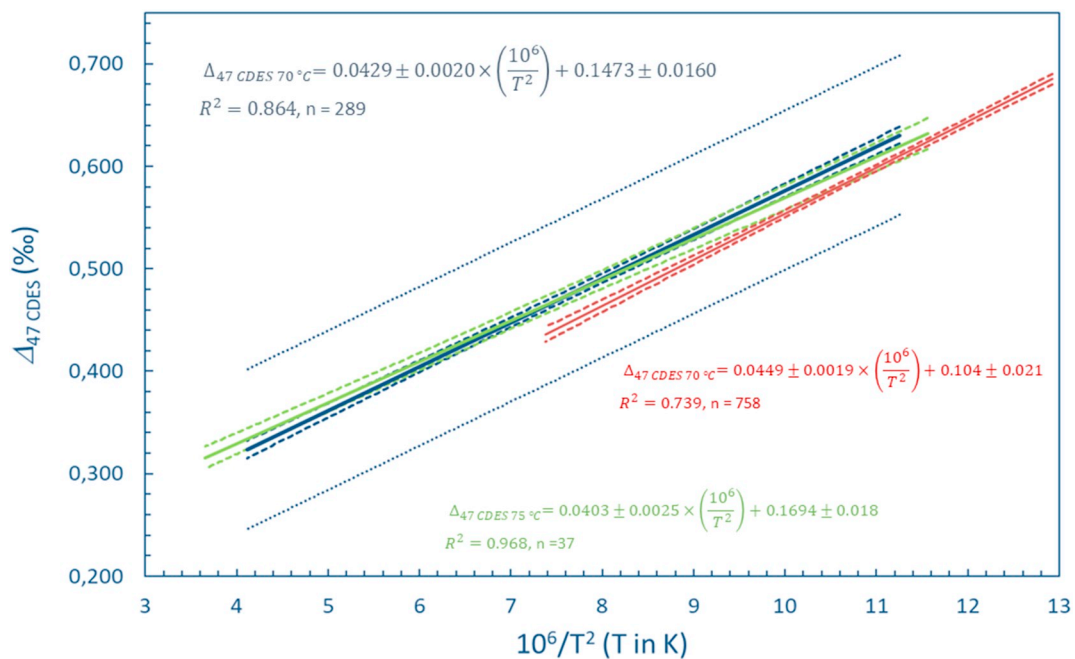
Fig. 6. The (proto-)dolomite specific Δ_{47}-T calibration of this study is displayed as dark blue line embedded in its narrow dashed 95% confidence and wider blue pointed 95% prediction envelopes. The linear regression overlaps with the (proto-)dolomite calibration of Winkelstern et al. (2016) reevaluated with new IUPAC parameters in Petersen et al. (2019) displayed in green with 95% confidence envelopes, but both of them lie above the calcite specific Δ_{47}-T calibration of the ETH (Kele et al. (2015) re-evaluated in Bernasconi et al. (2018)) as red line with narrow 95% confidence envelope for 70 °C acid digestion. Each of the Δ_{47}-T calibrations is displayed for their used acid reaction temperature and is based on the number of individual measurements indicated below each regression equation. (For interpretation of the references to colour in this figure legend, the reader is referred to the web version of this article.)

available. This was based on the assumption that the clumped isotope fractionation during acid digestion is identical for the two minerals (e.g. Millán et al., 2016; Winkelstern and Lohmann, 2016). Ferry et al. (2011) on the other hand, used another approach: they added a correction factor of 0.02 ‰ and used the theoretical calibration of Guo et al. (2009) to calculate formation temperatures of dolomites. The significant difference we observe in this study between the calcite and dolomite calibration measured with the same methodology, therefore, suggest that published estimates of temperatures of dolomite formation may have to be reevaluated. This reevaluation will also have to take into consideration that the original data in all publications before 2017 were not processed using the IUPAC parameters, which also can lead to significant changes in calculated compositions (Daëron et al., 2016). The effect on the recalculated temperatures in older publications is difficult to predict without a full recalculation that includes all heated and equilibrated gases measured with the samples (Petersen et al., 2019).

4.1.2. Comparison to other published dolomite calibrations: phosphoric acid fractionation

In recent years, two dolomite specific Δ_{47}-T calibrations were published, one of them reacting dolomite at 75 °C (Winkelstern et al., 2016) and the other at 90 °C (Bonifacie et al., 2017). The comparison of calibrations established in different laboratories, however, remains challenging, because of many factors: the lack of carbonate standards to compare across laboratories, the fact that clumped isotope data pre-2016 are not calculated using the "Brand parameters" and the different phosphoric acid fractionation factors used in different laboratories to project data produced at high reaction temperatures to 25 °C (Bernasconi et al., 2018; Petersen et al., 2019). For instance, Defliese et al. (2015) determined that temperature dependence of the acid fractionation factor for dolomite between 25 and 90 °C is identical to the one of calcite whereas Murray et al. (2016) observed a temperature dependence significantly steeper for dolomite. Thus, using the steeper temperature relationship of the acid fractionation for dolomite to

project data to 25 °C would lead to a larger difference to calcite at acid reaction temperatures below 90 °C than what would be observed using the Defliese et al. (2015) relationship.

The only study which determined the absolute Δ_{47} acid fractionation at 70 °C using various carbonate minerals with a stochastic isotope distribution is that of Müller et al. (2017a). This study showed that at 70 °C the acid fractionation of dolomite is 29 ppm larger than the one of calcite. Our new calibration allows now to determine if the acid fractionation is the cause of the observed differences.

The calcite specific Δ_{47}-T calibration produced at the ETH and reproduced in three recent studies at different laboratories using a Kiel carbonate device at 70 °C (Breitenbach et al., 2018; Piasecki et al., 2019) and a common acid bath extraction line at 90 °C (Peral et al., 2018) for planktic and benthic foraminifera clearly lie below our new dolomite calibration by about 30 ppm, but with slopes that are within error of each other. The difference between the intercepts of the dolomite and calcite calibrations produced at the ETH can be explained by the differences in the absolute Δ_{47} acid fractionation between calcite and dolomite of 0.029 ‰ (Müller et al., 2017a). However, when recalculating the data from Müller et al. (2017a) with the new accepted ETH standard values of Bernasconi et al. (2018) calculated with the IUPAC parameters, rather than those of Meckler et al. (2014), the difference in phosphoric acid fractionation between calcite and dolomite becomes 0.04 ‰ (see Tables 4, S3). This would suggest a slightly different (0.01 ‰) clumped isotope acid fractionation for dolomite and calcite at a specific temperature. A recent study analyzed the oxygen isotope and Δ_{47} composition of extremely slow growing carbonates, one is a calcite coating found in a cave lake, Laghetto Basso, Italy and the other sample is as well a subaques mammillary calcite coating from the Devils Hole cave, USA (Daëron et al., 2019). This study, although only constrained with a two point Δ_{47} temperature calibration, showed a small offset to other calcite calibrations with lower Δ_{47} values for equal formation temperatures. The authors used their observation as potential evidence that most calcites formed at surface conditions are out of isotopic equilibrium. The observed offset of their calibration to our new

Table 4
Heated carbonates (Δ_{47} acid fractionations).

Identifier	$\delta^{13}C_{VPDB}$ (‰)	$\delta^{18}O_{VPDB}$ (‰)	$\Delta_{47 \; CDES \; 70°C}$ (‰)	#
Aragonites				
Billin 1 (H)	3.10 ± 0.01	−8.36 ± 0.01	0.165 ± 0.009	64
Billin 2 (H)	−10.99 ± 0.06	−5.59 ± 0.05	0.176 ± 0.013	38
Average			0.169 ± 0.007	102
Calcites				
MS 2 (H)	2.06 ± 0.01	−1.91 ± 0.02	0.183 ± 0.008	88
ETH-4 (H)	−10.20 ± 0.01	−18.72 ± 0.02	0.187 ± 0.008	107
Merck (H)	−41.91 ± 0.02	−15.62 ± 0.01	0.192 ± 0.009	66
Average			0.187 ± 0.005	258
Dolomites				
Rodolo (H)	−3.89 ± 0.02	1.78 ± 0.04	0.229 ± 0.009	91
Sansa (H)	1.29 ± 0.02	−3.68 ± 0.04	0.226 ± 0.010	57
Average			0.227 ± 0.007	148

All uncertainties are displayed at the 95% CL.

(proto-)dolomite Δ_{47} temperature calibration is with 0.04 ‰ very similar to the offset between the absolute Δ_{47} acid fractionations of calcite and dolomite of Müller et al. (2017a) re-evaluated with the new IUPAC parameters in our study (see Table 4). This would be evidence that the clumped isotope composition of our (proto-)dolomites is in equilibrium to their actual formation temperature.

In general the almost identical slopes for the calcite calibrations discussed above with the dolomite one (this study) and the siderite calibration of van Dijk et al. (2019) supports the idea that the temperature dependence of clumped isotopes is the same for all minerals (Bonifacie et al., 2017; van Dijk et al., 2019). The offset of about 30 ppm between calcite and dolomite as well as the offset observed between siderite and calcite for the siderites reacted at 70 °C (van Dijk et al., 2019), however, shows the necessity to treat different minerals digested at 70 °C differently than calcites. For example for a dolomite formed at 25 °C we would obtain 6 °C colder temperatures if calculated as a calcite and for one formed at 80 °C we would obtain 12 °C colder temperatures, which further impacts the calculated $\delta^{18}O$ of the fluid source. An offset between the Δ_{47}-T relationship of dolomite and calcite was also predicted by theoretical calculations of Guo et al. (2009), however, the offset was of opposite sign of what we observe experimentally.

In Fig. 6 we plotted linear regressions obtained from the individual measurements in our new (proto-)dolomite dataset ($n = 289$), the ETH calcite dataset ($n = 758$) analyzed at same laboratory conditions (Kele et al., 2015) and the (proto-)dolomite dataset ($n = 37$) for common acid bath digestion at 75 °C of Winkelstern et al. (2016), with the latter two being fully re-evaluated with the new IUPAC parameters in Bernasconi et al. (2018) and Petersen et al. (2019), respectively. The datasets were evaluated for their values at the original acid digestion temperature, ETH dolomite and calcite samples for 70 °C reaction temperature and the Winkelstern et al. (2016) dataset for 75 °C reaction temperature, using their newly recommended ACC of 0.072 ‰ of Petersen et al. (2019). Although, we did not use a "York" like approach with assigning uncertainties to y and x observations to construct the linear regressions with their uncertainties at the 95% confidence interval as in Bonifacie et al. (2017) or Petersen et al. (2019), we obtain identical results with the linear regression tool in Excel. Although we agree that taking into account the temperature uncertainties would be the proper way to propagate all present uncertainties, our dataset evaluation reveals neglectable difference for the Winkelstern et al. (2016) dataset, that are at the fourth and third digit for the slope and intercept published in Petersen et al. (2019). We interpret this in the way that for bigger calibration datasets with higher sample replication and many different samples formed at different temperatures over a wide temperature range, assigning uncertainties on both regression variables has minor influence as the temperature uncertainty at the $10^6/T^2$ scale becomes neglectable at higher temperatures as it is the case for most of our calibration samples. In Fig. 6 we plotted for the three calibration datasets the 95% confidence interval, demonstrating with the narrow range how well constraint these linear regressions for the individual calibrations are. For our new (proto-)dolomite calibration we also added the 95% prediction interval, the blue dotted envelops, which shows a much wider range that meets our analytical uncertainty for an individual measurement. On Fig. 6 it is visible that the two dolomite calibrations are above the ETH calcite one and we compared the significance of differences in the slopes and intercepts of the Winkelstern study with respect to the two ETH calibrations with the GraphPad Prism 7.01 software (after Zar, 1984; see weblink https://www.graphpad.com/guides/prism/7/curve-fitting/index.htm?Reg_Comparingslopesandintercepts.htm). The slopes of the two (proto-)
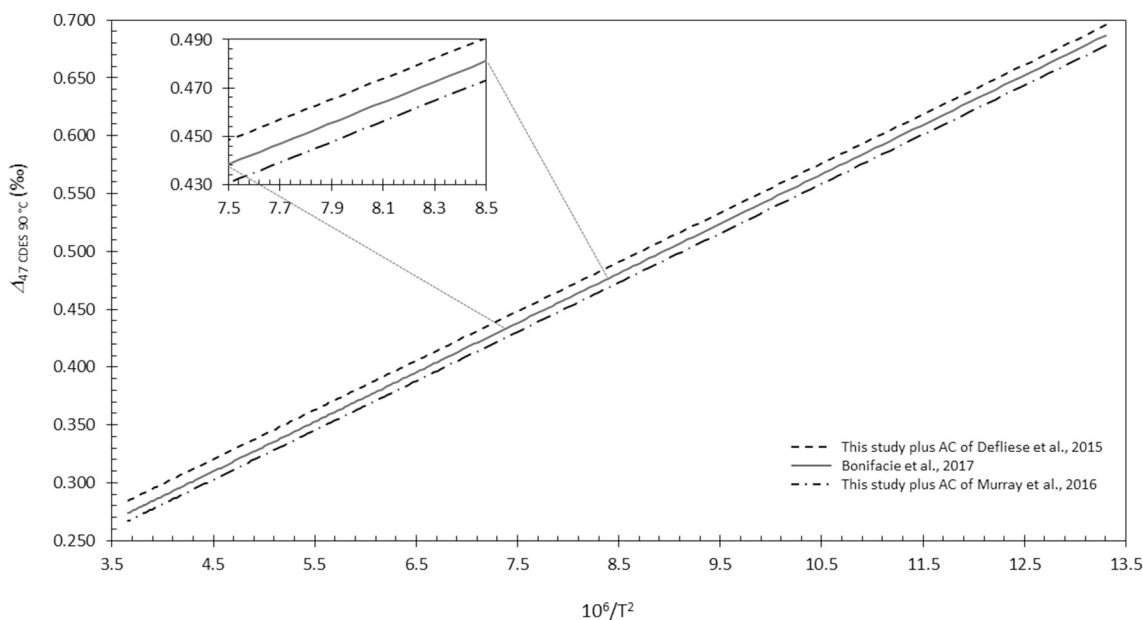
Fig. 7. The new dolomite specific Δ_{47}-T calibration was projected to 90 °C acid digestion temperature using the AC of 0.0204 ‰ (Defliese et al., 2015, dashed black line), the AC of 0.0380 ‰ (Murray et al., 2016, black line with dashes and dots) to compare it directly to the dolomite calibration Bonifacie et al. (2017) (grey line in the middle). The top left box shows a blow-up to better visualize the offsets at the temperature range between 70 and 92 °C.

dolomite calibrations are statistically identical with a *p* value of 0.1696 and subsequent pooling of the slopes to test eventual differences in the y-intercept reveal also a significant overlap with a p value of 0.7323. Whereas the slopes of the two ETH calibrations are not significantly different, but the intercepts are, the statistical evaluation of the Winkelstern et al. (2016) dataset reevaluated in Petersen et al. (2019) for 75 °C acid digestion is significantly different in slope (p value of 0.0395) and intercept to the re-evaluated ETH calcite calibration dataset. This difference would even increase when adding a ACC correction for the small difference in their reaction temperatures.

The (proto-)dolomite specific Δ_{47}-temperature calibration of Bonifacie et al. (2017) is based on 12 different samples formed at temperatures between 25 and 350 °C with a total of 67 individual measurements and contains one sample from Lagoa Vermelha and another one of a neighbouring lagoon (Brejo do Espinho) that formed under similar conditions as the ones we used in this study. In their study Bonifacie et al. (2017) reacted 5 mg samples with 104% phosphoric acid in a common acid bath at 90 °C and obtained a linear regression of $\Delta_{47\ CDES\ 90°C} = (0.0428 \pm 0.0033) * 10^6/T^2 + (0.1174 \pm 0.0248)$. This slope is identical to the slope of 0.0428 in this study and thus allows to directly evaluate the clumped isotope acid fractionation correction required to compare Δ_{47} measurements of the different laboratories to each other. For a direct comparison between the two studies we can compare the natural samples of Lagoa Vermelha where we obtained a $\Delta_{47\ CDES\ 70°C}$ of 0.637 ± 0.022 ‰ for the upper one (LV 15 cm, 16 replicates) and Bonifacie et al. (2017) obtained a $\Delta_{47\ CDES\ 90°C}$ of 0.591 ± 0.022 ‰ (4 replicates) for their surface sample, an offset of 0.046 ‰. The average offset between our two sediment samples from Lagoa Vermelha and their two Brazilian lagoonal samples (CVLV and CVBE of their Table 2) is approximately 0.029 ‰. In Fig. 7 we plotted the temperature calibration of Bonifacie et al. (2017) with the $\Delta_{47\ CDES\ 90°C}$ against the inverse temperature and applied the two differing published dolomite specific acid fractionations (Defliese et al., 2015; Murray et al., 2016) to project our dolomite data to 90 °C acid digestion temperature.

Applying an acid fractionation correction (AC) of 0.0204 ‰ derived from Defliese et al. (2015), which observed no significant differences between dolomite and calcite, our dolomite calibration lies parallel

with an offset of about 10 ppm above the one of Bonifacie et al. (2017) (see Fig. 7). Whereas with the AC of 0.0380 ‰ from Murray et al. (2016), which observed a much steeper temperature relationship for dolomite compared to calcite, our calibration shifts down to about 8 ppm below the one of Bonifacie et al. (2017). The AC effectively needed to put the calibrations on the same level is an AC of approximately 0.030 ‰, which is somewhere in between the values of Defliese et al. (2015), and that of Murray et al. (2016), and corresponds to the observed offset between our lagoonal proto-dolomite concretions and the ones of Bonifacie et al. (2017). An additional uncertainty in this comparison is the fact that the Bonifacie et al. (2017) was not corrected for the "IUPAC" parameters, thus the exact difference remains unclear until the data from Bonifacie are recalculated.

The above discussion shows that applying an acid fractionation correction for Δ_{47} analyses on dolomite can result in large uncertainties and produce erroneous temperature estimates. Ideally laboratories should apply temperature calibrations based on dolomite samples that were acid digested at the same temperature as already recommended by Bonifacie et al. (2017). The only way to remove these uncertainties for dolomite measurements is the use of dolomite reference materials in addition to the calcite standards that are used to transfer the data to the CDES. The regular analysis of dolomite standards would drastically reduce the uncertainties arising from mineral specific acid fractionation correction and uncertainties arising from small differences in sample purification procedures and data processing across laboratories (see also Bernasconi et al., 2018). This would be valuable not only for clumped isotopes but also for oxygen isotopes as well, as there are also uncertainties in oxygen isotope fractionation with different preparation systems. The international NIST SRM 88b is such an example of a dolomite that is often analyzed and two potential dolomite reference materials are presented below.

4.1.3. Effect of crystallographic ordering on clumped isotope fractionation

Our dolomite specific Δ_{47}-T calibration shows an almost identical slope as the calibration of Bonifacie et al. (2017), which also used a mixture of high temperature stoichiometric poorly- to well-ordered dolomites and lower temperature proto-dolomites. Their high temperature samples were synthesized by placing calcite or aragonite in Ca-
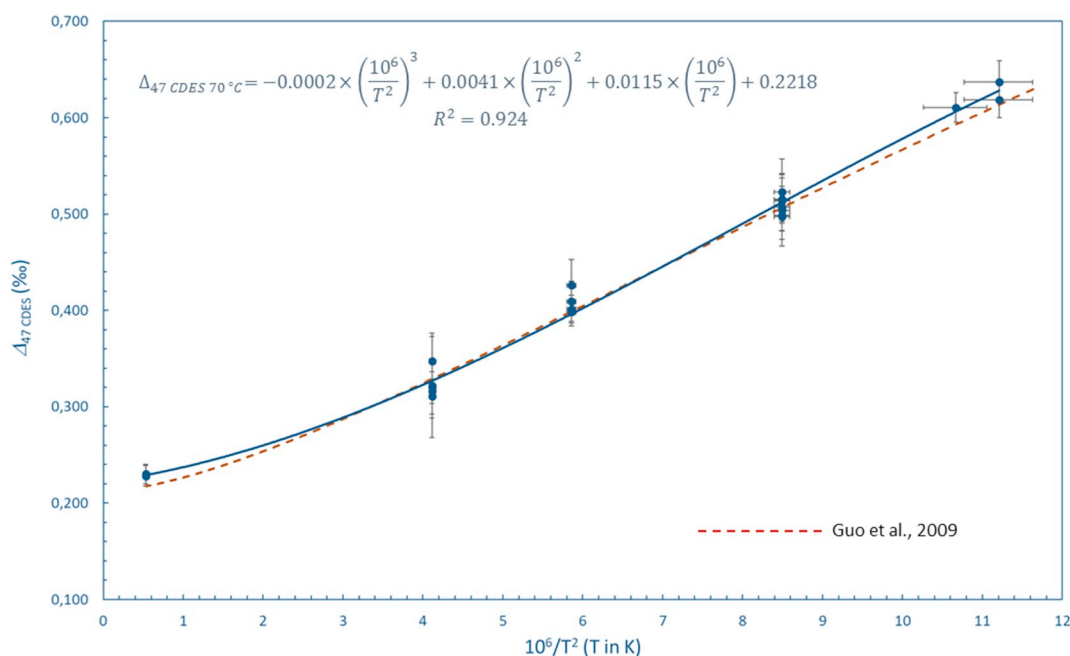

$$\Delta_{47\ CDES\ 70\,°C} = -0.0002 \times \left(\frac{10^6}{T^2}\right)^3 + 0.0041 \times \left(\frac{10^6}{T^2}\right)^2 + 0.0115 \times \left(\frac{10^6}{T^2}\right) + 0.2218$$
$$R^2 = 0.924$$

Fig. 8. The dark blue line corresponds to the third order polynomial fit (equation in figure) through all of our (proto-)dolomite calibration samples between 25 and 1100 °C and the dashed brown line corresponds to the theoretical dolomite Δ_{47}-T relationship from Guo et al. (2009) for 25 °C acid digestion temperature. (For interpretation of the references to colour in this figure legend, the reader is referred to the web version of this article.)

Mg-(Na)-Cl solutions in stainless steel reactor vessels that were heated for several days at the corresponding experiment temperature of 100 to 350 °C (Horita, 2014 and Bonifacie et al., 2017). Thereby the starting carbonate phase converts first into high-Mg calcite, then into poorly-ordered dolomite to well-ordered near stoichiometric dolomite. This is similar to dolomite formation in our experiments, except that we did not use a solid carbonate starting phase. For their low temperature samples Bonifacie et al. (2017) used samples from the same Brazilian hypersaline lagoon (Vasconcelos and McKenzie, 1997) we have used as well as bacterially-mediated precipitated proto-dolomites that were originally used to calibrate the oxygen isotope fractionation between dolomite and the water (Vasconcelos et al., 2005). At the intermediate temperature of 80 °C Bonifacie and colleagues precipitated proto-dolomite from mixing solutions of $MgSO_4$, $Ca(NO_3)_2*4H_2O$ and Na_2CO_3 and keeping this mixture for > 41 days in a temperature controlled water bath. Despite the different methods of forming (proto-)dolomites, the differing degrees of ordering and the different acid digestion temperatures used in the two studies, the slopes of our calibrations are statistically indistinguishable. Therefore, we conclude that there is no difference in the temperature dependence of Δ_{47} between ordered stoichiometric dolomites and so-called proto-dolomite, or, if such differences exist, they are well below the current analytical uncertainty. We are aware that our samples are not ideal stoichiometric ordered dolomite, however, the presence of the ordering peaks in the natural samples, the 140 and 220 °C samples is typical for poorly ordered to well-ordered, in most cases stoichiometric or very close to stoichiometric dolomite. Therefore we expect no or only minor differences to an ideal ordered stoichiometric dolomite as those found in the geologic record. The minor differences to reported slopes of recent calcite calibrations (e.g. Bonifacie et al., 2017; Bernasconi et al., 2018; Breitenbach et al., 2018; Kelson et al., 2017; Peral et al., 2018; Daëron et al., 2019) or a new siderite calibration (van Dijk et al., 2019) strongly suggests that the slope of the clumped isotope temperature relationship is identical for different carbonate minerals. In contrast, the intercepts of the calibrations differ for the different minerals due to the difference in phosphoric acid fractionation. This has to be taken into account, especially at lower acid digestion temperatures where these effects may have a larger impact (Murray et al., 2016; Müller et al., 2017a). Additional measurement of various dolomite and calcite standards would enable a better and more direct data comparison to solve this discrepancy.

In Fig. 8 we additionally added the two dolomite samples heated to 1100 °C to expand the dolomite Δ_{47}-T relationship at elevated temperatures that can prevail in lower crustal environment or where magmatic intrusions penetrate sedimentary rocks (e.g. Lloyd et al., 2017; Ryb et al., 2017). The resulting Δ_{47}-T relationship is a third order polynomial fit that is largely identical to the theoretical dolomite calibration for 25 °C acid reaction temperature of Guo et al. (2009) displayed as grey dashed line in Fig. 8. Although the theoretical dolomite calibration of Guo et al. (2009) was calculated for 25 °C acid digestion temperature it fits well to our calibration without any correction and the small differences below 70 °C and above 500 °C might be due to the fact that we do not have enough different high temperature samples between the 220 °C and the 1100 °C samples as well as at low temperatures for a better higher order polynomial fitting. The linear regression for the dolomite specific Δ_{47}-T calibration for 70 °C acid digestion fits the theoretical dolomite calibration better in the low temperature range. The striking resemblance between our polynomial fit and the theoretical calculations show that both relationships can be applied for dolomites exposed to temperatures above ~400 °C in natural environments and supports our obtained (proto-)dolomite specific Δ_{47}-temperature relationship and the ones reported in Winkelstern et al. (2016) reevaluated in Petersen et al. (2019) and the one in Bonifacie et al. (2017). On the other hand, the observation that our calibration for 70 °C acid digestion temperature (without AFF) lies on their theoretical line for 25 °C acid digestion might be due that they underestimate the

dolomite specific Δ_{47} acid fractionation or could be just coincidence. Once more the regular analysis of dolomite standards would help to correct for offsets between laboratories digesting the carbonates at different reaction temperatures allowing laboratories without own temperature calibration the application of dolomite specific Δ_{47}-T calibrations with more confidence.

4.2. Oxygen isotope fractionation between (proto-)dolomites and water

Dolomite is known to have a different oxygen isotope fractionation to water compared to other carbonate minerals and its temperature dependency was thoroughly studied since many decades (e.g. Northrop and Clayton, 1966; Fritz and Smith, 1970; Matthews and Katz, 1977; Zheng, 1999; Vasconcelos et al., 2005; Horita, 2014). Unfortunately all of these studies faced the challenge that in laboratory at temperatures below 100 °C it becomes difficult to synthesize dolomite, although naturally occurring dolomite samples in most cases formed at lower temperatures (e.g. via mixing of fluids, as diagenetic replacement phase or biologically mediated primary precipitate, see Warren (2000) for a review). Some earlier studies produced dolomite at high temperatures > 100 °C and extrapolated their results to lower temperatures (Northrop and Clayton, 1966; Matthews and Katz, 1977). Other studies precipitated with or without the help of microorganisms a carbonate phase that is not perfectly stoichiometric dolomite (Gregg et al., 2015), but this proto-dolomite phase was formed at near surface temperatures (e.g. Fritz and Smith, 1970; Vasconcelos et al., 2005).

While these proto-dolomites are not well ordered, they show properties that distinguish them from calcite. The cultures of Vasconcelos et al. (2005) produced a mixture of calcite and proto-dolomite and before measurement they dissolved the calcite with EDTA, thus the Mg rich phase that has the main d(104) XRD peak in the position of a dolomite, was more resistant to dissolution than all carbonate phases with lower Mg concentration. We consider this a good indication that these phases, although not well ordered, are not very high magnesium calcites (Kaczmarek and Thornton, 2017), but poorly ordered dolomites.

Another approach to overcome the difficulty of precipitating low temperature dolomites was the theoretical modelling of the dolomite water oxygen isotope fractionation of Zheng (1999). Other studies, including ours, merged results from stoichiometric poorly to well-ordered dolomites formed at temperatures above 140 °C with results from proto-dolomites formed at temperatures down to 70 °C (experiments down to 80 °C in Horita, 2014). A recent study of Murray and Swart (2017) discussed and evaluated the existing oxygen isotope calibrations using dolomites from the Bahamas, on which they applied clumped isotope thermometry. In Fig. 1 they show that for dolomite formed at 25 °C the calculated $\delta^{18}O$ of the fluid source can vary by up to 3.6 ‰ depending on which calibration is used. Murray and Swart evaluated the various calibrations, by calculating the $\delta^{18}O_{fluid}$ from the Δ_{47} temperature estimates and the corresponding expected $10^3 ln\alpha_{Dolomite-Water}$ to further test if the results are consistent with existing dolomitization models for the Bahamian dolomites. In their study, they favored the application of the temperature relationship of Matthews and Katz (1977) for the Bahamian dolomites that presumably formed at temperatures between 15 and 35 °C. They discarded the low temperature dolomite calibrations covering this temperature range arguing that they were based on proto-dolomites or very-high Mg-calcite samples (Fritz and Smith, 1970; Vasconcelos et al., 2005). However, these two calibrations give very comparable results to the Matthews and Katz (1977) calibration, suggesting that the proto- or poorly ordered dolomites have a very similar oxygen isotope fractionation to ordered dolomites.

The direct comparison of the published studies on the temperature dependency of the oxygen isotope fractionation between dolomite and water is complicated by the fact that different studies used different phosphoric acid fractionation factors. In our study, we use the acid fractionation factor correction for dolomite of Rosenbaum and

Sheppard (1986), like the two most recent studies of Vasconcelos et al. (2005) and Horita (2014). In contrast, Northrop and Clayton (1966) used a correction factor of 1.01090 for a 25 °C acid reaction, Fritz and Smith (1970) used the calcite acid fractionation factor of 1.01008 (Sharma and Clayton, 1965) and Matthews and Katz (1977) use a factor of 1.01110 for 25 °C from Friedman and O'Neil (1977). Further uncertainties might originate from the oxygen isotope analyses of the water when comparing studies published during almost half a century. In Fig. 9 we compiled the oxygen isotope fractionation between (proto-)dolomites and water of this study with the two most recently published temperature relationships (Vasconcelos et al., 2005; Horita, 2014) together with the temperature relationship of Matthews and Katz (1977) recommended in the study of Murray and Swart (2017). For Matthews and Katz (1977) we applied a correction factor of −0.68 ‰ to correct for the different acid fractionation correction used. The factor of −0.68 ‰ is the difference between the acid fractionation factor used by Matthews and Katz (1977) and the one for 25 °C acid digestion of Rosenbaum and Sheppard (1986). From Fig. 9 it appears that our new experimental data overlap with those of Vasconcelos et al. (2005) and Horita (2014), whereas the Matthews and Katz (1977) calibration is slightly below the data compilation over the entire temperature range. Because of the uncertainties in the $\delta^{18}O_{H2O}$ of water from Lagoa Vermelha we do not include the oxygen isotope fractionations of these two natural samples in the temperature calibration in Fig. 9. The XRD pattern of the (proto-)dolomites used in Horita (2014) are very similar to ours, although they used various carbonate seeds to synthesize the dolomites. Whereas our 70 °C samples match well their temperature dependent (proto-)dolomite water oxygen isotope fractionation, our samples at 140 and 220 °C show more scatter. In case of the 220 °C the two samples with larger oxygen isotope fractionation could be explained by in two ways, first it could be that they inherited the isotope composition of a more poorly ordered dolomite (like sample Leeds 34, which we did exclude here) that formed at lower temperature during the heating stage of the experiment or that the degree of ordering affects the oxygen isotope equilibrium with the water. A third explanation could be that some of the solution leaked/evaporated out of the experiment container slightly enriching the remaining solution in the heavier ^{18}O (these would be then the two samples matching Horita's data Leeds 84 and 85). In case of the samples synthesized at 140 °C

suspiciously only the one sample of the shortest experiment, the proto-dolomite Leeds 21 matches that data of Horita, whereas the others show larger fractionations. On the other side our proto-dolomite samples formed at 70 °C bridge nicely the existing gap of the two datasets of Vasconcelos et al. (2005) and Horita (2014).

The study of Horita (2014) contains samples that cover a temperature range from 80 to 350 °C, whereas the study of Vasconcelos et al. (2005) covers a temperature range of 25 to 45 °C with a slightly more shallow temperature relationship. If the results of the proto-dolomites precipitated between 25 and 79 °C of Fritz and Smith (1970) are corrected for the difference of their applied acid fractionation at 25 °C, their calibration line is parallel to but slightly below (~1 ‰) the one of Vasconcelos et al. (2005).

In spite of the possible limitations discussed above, we propose to combine the results of the three studies to derive a more accurate temperature dependence of the water-(proto-)dolomite oxygen isotope fractionation because it is based on more data points and covers a wide temperature range of 25 to 350 °C (see Fig. 9). Based on observations from the statistical evaluation of Fernandez et al. (2017) of existing Δ_{47}-T calibrations that more samples covering a wider temperature range lead to more robust calibrations we therefore recommend to use this combined $10^3 ln\alpha_{Dolomite-Water}$-T relationship.

$$10^3 \ln \alpha_{Dolomite-Water} = 2.9923 \pm 0.0557 \times (10^6/T^2) - 2.3592 \pm 0.4116$$

to calculate the $\delta^{18}O$ of the fluid source of unknown samples. This makes poorly constrained extrapolations from calibrations based on high temperature dolomites to lower temperatures unnecessary.

4.3. New dolomite reference materials for improved inter-laboratory comparison of carbon, oxygen and clumped isotopes

The comparison of the new dolomite specific Δ_{47}-T calibration of this study for 70 °C acid digestion with the calibration of Bonifacie et al. (2017) produced at 90 °C shows that the slope of the calibration is statistically indistinguishable, and similar to calcites and siderites, indication that all carbonates have a common calibration. However, there is a discrepancy in the intercept of the calibration due to poor understanding of the temperature dependence of the AFF for dolomite and possibly due to the use of the IUPAC parameters in the calculations. In
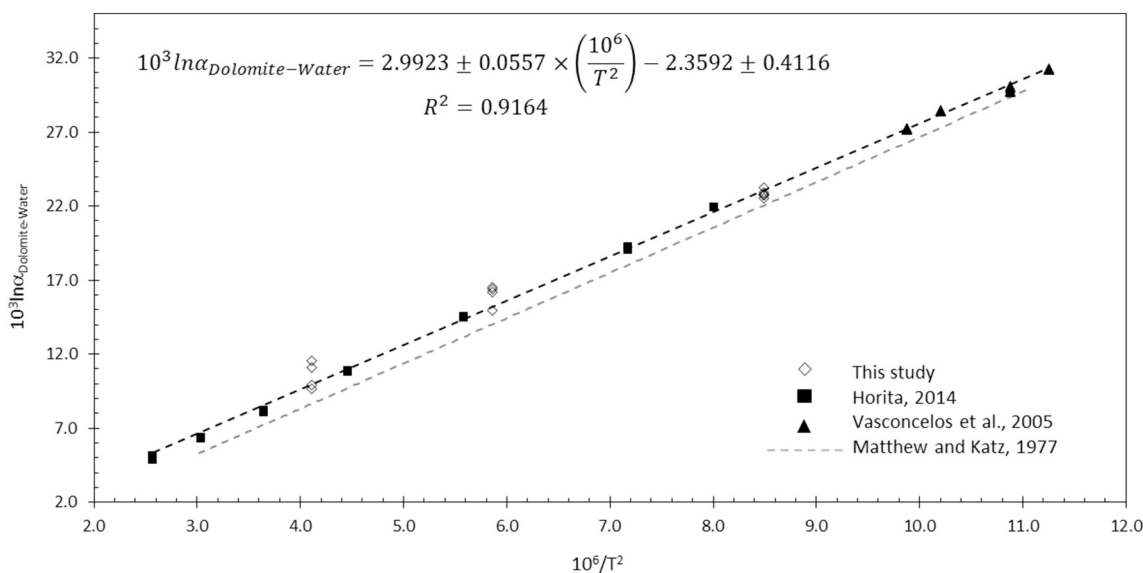

Fig. 9. The oxygen isotope fractionation between (proto-)dolomites and precipitation solutions of the individual synthesized samples of this study (70, 140 and 220 °C, black hollow diamonds), samples of Horita (2014) (black squares) and of Vasconcelos et al. (2005) (black triangles) are plotted against the inverse temperature. Combination of these three datasets resulted in the black dashed line giving the displayed linear relationship and covers a temperature range from 25 to 350 °C. As dashed grey line we also plotted the temperature relationship of Matthews and Katz (1977) (corrected for the acid digestion factor of Rosenbaum and Sheppard (1986) for consistent data treatment) lying slightly below our combined one.

addition, we observed a larger difference to the calibration of Winkelstern et al. (2016) (difference in slope and intercept) although it was realized with acid digestion temperature of 75 °C, closer to ours and was recalculated with the IUPAC parameters (Petersen et al., 2019). This points to other unknown factors in the sample preparation and/or data standardization as cause for the discrepancy. These observed differences together with the inconclusive comparisons to other dolomite Δ_{47}-fluid inclusion studies that used calcite specific Δ_{47}-T calibrations (Came et al., 2017; Honlet et al., 2017) underline the urgent need of dolomite reference materials to reduce the uncertainties between laboratories. Simultaneous measurements of multiple dolomite standards with different bulk isotope composition, different degree of ordering and different Δ_{47} allows to detect differences due to scale compression, background correction or calculations to transfer the isotope results to the CDES (see Bernasconi et al. (2018) for a detailed discussion of the advantages of carbonate standards). In addition, these dolomite reference materials, will also help solving uncertainties in oxygen isotope fractionation. We propose three possible reference materials (XRD patterns displayed in Fig. 3 and Table 3) that have a range of compositions and are available in large amounts for distribution. Besides the already available NIST SRM 88b dolomite standard ($\Delta_{47\ CDES\ 70°C}$ of 0.522 ± 0.022 ‰) that is distributed by the National Institute of Standards and Technology (Gaithersburg, MD, USA), we propose two potentially new dolomite reference materials, the lacustrine low temperature dolomite "Rodolo" a stoichiometric, but poorly ordered dolomite ($\Delta_{47\ CDES\ 70°C}$ of 0.632 ± 0.006 ‰) and the warmer well-ordered stoichiometric dolomite "Sansa" ($\Delta_{47\ CDES\ 70°C}$ of 0.526 ± 0.014 ‰), which is the product of diagenetic alteration of a primary early Triassic marine carbonate (Table 3). The Rodolo and Sansa can be obtained directly from Stefano Bernasconi (stefano.bernasconi@erdw.ethz.ch). Rodolo and Sansa were also analyzed for their Δ_{47} in the laboratory of the MIT with a Nu Perspective mass spectrometer coupled to a Nu Carb device by Kristin D. Bergmann and reproduced well the results of the ETH laboratory (see Bernasconi et al., 2018).

5. Conclusions

We propose a new (proto-)dolomite specific Δ_{47}-T calibration for 70 °C acid digestion covering a temperature range from 25 to 1100 °C, based on 22 different (proto-)dolomite samples that formed at known temperatures and consists of a total of 435 individual measurements. This new dolomite calibration has identical slope but an offset of about 30 ppm to the one of Bonifacie et al. (2017) for 90 °C digestion. This offset corresponds to the dolomite isotope acid fractionation correction between 70 °C and 90 °C reaction.

The 30 ppm difference lies between the one predicted by Defliese et al. (2015) and the one by Murray et al. (2016). However, the offset of 30 ppm could potentially change if the dataset of Bonifacie et al. (2017) is recalculated with the newly recommended IUPAC parameters for ^{17}O correction (also referred as "Brand" parameters).

The new (proto-)dolomite specific Δ_{47}-T calibration shows a clear offset of about 30 ppm in the temperature range of 5 to 95 °C to the calcite specific calibration produced under identical conditions in the same laboratory (Bernasconi et al., 2018). The slopes of both calibrations are within uncertainties (0.0428 ± 0.0020 for dolomite vs. 0.0449 ± 0.0019 for calcite). The offset between the two calibration sets corresponds to the different absolute Δ_{47} acid fractionations of dolomite and calcite already observed in Müller et al. (2017a).

We propose a new (proto-)dolomite-water oxygen fractionation equation valid for temperatures between 25 and 350 °C based on a compilation from samples from this study, Vasconcelos et al. (2005) and Horita (2014).

We propose three reference materials to improve interlaboratory comparability of clumped and oxygen isotope data of dolomites.

The observed differences between the calcites and dolomites and the uncertainties in correcting Δ_{47} and $\delta^{18}O$ analyses of dolomites for

different acid digestion temperatures underline the necessity of using dolomite specific Δ_{47}-T calibrations, ideally constructed at identical sample reaction temperatures. The regular analysis of dolomite reference materials would also enable the use of (proto-)dolomite specific Δ_{47}-T calibrations done in other laboratories and in general would allow a much better data comparison between different laboratories.

Appendix A. Supplementary data

Supplementary data to this article can be found online at https://doi.org/10.1016/j.chemgeo.2019.07.014.

References

Assonov, S., Brenninkmeijer, C., 2003. A redetermination of absolute values for $^{17}R_{VPDB-CO_2}$ and $^{17}R_{VSMOW}$. Rapid Commun. Mass Spectrom. 17, 1017–1029.

Baertschi, P., 1976. Absolute ^{18}O content of standard mean ocean water. Earth Planet. Sci. Lett. 31, 341–344.

Bahniuk, A., McKenzie, J.A., Perri, E., Bontognali, T.R.R., Vögeli, N., Rezende, C.E., Rangel, T.P., Vasconcelos, C., 2015. Characterization of environmental conditions during microbial Mg-carbonate precipitation and early diagenetic dolomite crust formation: Brejo do Espinho, Rio de Janeiro, Brazil. From In: Bosence, D.W.J., Gibbons, K.A., LeHeron, D.P., Morgan, W.A., Pritchard, T., Vining, B.A. (Eds.), Microbial Carbonates in Space and Time: Implications for Global Exploration and Production. vol. 418. Geological Society, London, pp. 243–259 Special Publications.

Barkan, E., Luz, B., 2005. High-precision measurements of $^{17}O/^{16}O$ ratios in H_2O. Rapid Commun. Mass Spectrom. 26, 2733–2738.

Bernasconi, S.M., Hu, B., Wacker, U., Fiebig, J., Breitenbach, S.F.M., Rutz, T., 2013. Background effects on Faraday collectors in gas-source mass spectrometry and implications for clumped isotope measurements. Rapid Commun. Mass Spectrom. 27, 603–612.

Bernasconi, S.M., Müller, I.A., Bergmann, K.D., Breitenbach, S.F.M., Fernandez, A., Hodell, D.A., Jaggi, M., Meckler, A.N., Millan, I., Ziegler, M., 2018. Reducing uncertainties in carbonate clumped isotope analysis through consistent carbonate-based standardization. Geochem. Geophys. Geosyst. 19, 2895–2914.

Berra, F., Jadoul, F., Anelli, A., 2010. Environmental control on the end of the Dolomia Principale/Hauptdolomit depositional system in the central Alps: coupling sea-level and climate changes. Palaeogeogr. Palaeoclimatol. Palaeoecol. 290, 138–150.

Bonifacie, M., Calmels, D., Eiler, J.M., Horita, J., Chaduteau, C., Vasconcelos, C., Agrinier, P., Katz, A., Passey, B.H., Ferry, J.M., Bourrand, J.-J., 2017. Calibration of the dolomite clumped isotope thermometer from 25 to 350 °C, and implications for a universal calibration for all (Ca, Mg, Fe)CO_3 carbonates. Geochim. Cosmochim. Acta 200, 255–279.

Bontognali, T.R.R., Vasconcelos, C., Warthmann, R.J., Bernasconi, S.M., Dupraz, C., Strohmenger, C.J., McKenzie, J.A., 2010. Dolomite formation within microbial mats in the coastal sabkha of Abu Dhabi (United Arab Emirates). Sedimentology 57, 824–844.

Bradley, W.F., Burst, J.F., Graf, D.L., 1953. Crystal chemistry and differential thermal effects of dolomite. Am. Mineral. 38, 207–217.

Brauchli, M., McKenzie, J.A., Strohmenger, C.J., Sadooni, F., Vasconcelos, C., Bontognali, T.R.R., 2016. The importance of microbial mats for dolomite formation in the Dohat Faishakh sabkha, Qatar. Carbonates Evaporites 31 (3), 339–345.

Breitenbach, S.F.M., Mleneck-Vautravers, M.J., Grauel, A.-L., Lo, L., Bernasconi, S.M., Müller, I.A., Rolfe, J., Gázquez, F., Greaves, M., Hodell, D.A., 2018. Coupled Mg/Ca and clumped isotope analyses of foraminifera provide consistent water temperatures. Geochim. Cosmochim. Acta 236, 283–296.

Bristow, T.F., Bonifacie, M., Derkowski, A., Eiler, J.M., Grotzinger, J.P., 2011. A hydrothermal origin for isotopically anomalous cap dolostone cements from south China.

Nature 474, 68–71.

Burns, S.J., McKenzie, J.A., Vasconcelos, C., 2000. Dolomite formation and biogeochemical cycles in the Phanerozoic. Sedimentology 47, 49–61.

Butler, G.P., 1969. Modern evaporite deposition and geochemistry for coexisting brines, the Sabkha, Trucial coast, Arabian Gulf. J. Sediment. Petrol. 39, 70–89.

Came, R.E., Azmy, K., Tripati, A., Olanipekun, B.-J., 2017. Comparison of clumped isotope signatures of dolomite cements to fluid inclusion thermometry in the temperature range of 73-176 °C. Geochim. Cosmochim. Acta 199, 31–47.

Chai, L., Navrotsky, A., Reeder, R.J., 1995. Energetics of calcium-rich dolomite. Geochim. Cosmochim. Acta 59, 939–944.

Chang, T., Li, W., 1990. A calibrated measurement of the atomic weight of carbon. Chin. Sci. Bull. 35, 290–296.

Coplen, T.B., 1996. Atomic weights of the elements 1995 (technical report). Pure Appl. Chem. 68, 2339–2359.

Coplen, T.B., Kendall, C., Hopple, J., 1983. Comparison of stable isotope reference samples. Nature 302, 236–238.

Daëron, M., Drysdale, R.N., Peral, M., Huyghe, D., Blamart, D., Coplen, T.B., Lartaud, F., Zanchetta, G., 2019. Most earth-surface calcites precipitate out of isotopic equilibrium. Nat. Commun. 10, 429.

Daëron, M., Blamart, D., Peral, M., Affek, H.P., 2016. Absolute isotopic abundance ratios and the accuracy of Δ_{47} measurements. Chem. Geol. 442, 83–96.

Dale, A., John, C.M., Mozley, P.S., Smalley, P.C., Muggeridge, A.H., 2014. Time-capsule concretions: Unlocking burial diagenetic processes in the Mancos Shale using carbonate clumped isotopes. Earth Planet. Sci. Lett. 394, 30–37.

Defliese, W.F., Hren, M.T., Lohmann, K.C., 2015. Compositional and temperature effects of phosphoric acid fractionation on Δ_{47} analysis and implications for discrepant calibrations. Chem. Geol. 396, 51–60.

Dennis, K.J., Affek, H.P., Passey, B.H., Schrag, D.P., Eiler, J.M., 2011. Defining an absolute reference frame for "clumped" isotope studies of CO_2. Geochim. Cosmochim. Acta 75, 7117–7131.

Do Nascimento, G.S., 2018. Influence of Climatic and Oceanographic Conditions on Biomineralization Processes in Hypersaline Coastal Lagoons (Rio de Janeiro – Brazil). Dissertation. ETH.

Dolomieu, D.G.D., 1791. Sur un genre de pierrres calcaires très-peu effervescentes avec les acides, & phosphorescentes par la collision. J. Phys. 39, 3–10.

Eiler, J.M., 2007. "Clumped-isotope" geochemistry-the study of naturally-occurring, multiply-substituted isotopologues. Earth Planet. Sci. Lett. 262, 309–327.

Fernandez, A., Müller, I.A., Rodríguez-Sanz, L., van Dijk, J., Looser, N., Bernasconi, S.M., 2017. A reassessment of the precision of carbonate clumped isotope measurements: implications for calibrations and paleoclimate reconstructions. Geochem. Geophys. Geosyst. 18, 4375–4386.

Ferry, J.M., Passey, B.H., Vasconcelos, C., Eiler, J.M., 2011. Formation of dolomite at 40-80 °C in the Latemar carbonate buildup, Dolomites, Italy, from clumped isotope thermometry. Geology 39, 571–574.

Friedman, I., O'Neil, J.R., 1977. Compilation of stable isotope fractionation factors of geochemical interest. In: Fleischer, M. (Ed.), Data of Geochemistry, Sixth edition. Geological Survey Professional Paper 440. pp. KK1–KK9.

Frisia, S., 1994. Mechanisms of complete dolomitization in a carbonate shelf: comparison between the Norian Dolomia Principale (Italy) and the Holocene of Abu Dhabi Sabkha. Int. Assoc. Sedimentol. Spec. Publ. 21, 55–74.

Fritz, P., Smith, D.G.W., 1970. The isotopic composition of secondary dolomites. Geochim. Cosmochim. Acta 34, 1161–1173.

García del Cura, A.M., Calvo, J.P., Ordóñez, S., Jones, B.F., Cañaveras, J.C., 2001. Petrographic and geochemical evidence for the formation of primary, bacterially induced lacustrine dolomite: La Roda 'white earth' (Pliocene, central Spain). Sedimentology 48, 897–915.

Ghosh, P., Adkins, J., Affek, H., Balta, B., Guo, W., Schauble, E.A., Schrag, D., Eiler, J.M., 2006a. ^{13}C-^{18}O bonds in carbonate minerals: a new kind of paleothermometer. Geochim. Cosmochim. Acta 70, 1439–1456.

Ghosh, P., Garzione, C.N., Eiler, J.M., 2006b. Rapid uplift of the Altiplano revealed through ^{13}C-^{18}O bonds in paleosol carbonates. Science 311, 511–515.

Given, R.K., Wilkinson, B.H., 1987. Dolomite abundance and stratigraphic age, constraints on rates and mechanisms of dolostone formation. J. Sediment. Petrol. 57, 1068–1078.

Goldsmith, J.R., Graf, D.L., 1958. Structural and compositional variations in some natural dolomites. J. Geol. 66, 678–693.

Graf, D.L., Goldsmith, J.R., 1956. Some hydrothermal syntheses of dolomite and protodolomite. J. Geol. 64, 173–186.

Grauel, A.L., Schmid, T.W., Hu, B., Bergami, C., Capotondi, L., Zhou, L., Bernasconi, S.M., 2013. Calibration and application of the "clumped isotope" thermometer to foraminifera for high-resolution climate reconstructions. Geochim. Cosmochim. Acta 108, 125–140.

Gregg, J.M., Bish, D.L., Kaczmarek, S.E., Machel, H.G., 2015. Mineralogy, nucleation and growth of dolomite in the laboratory and sedimentary environment: a review. Sedimentology 62, 1749–1769.

Guo, W., Mosenfelder, J.L., Goddard, I.I.I.W.A., Eiler, J.M., 2009. Isotopic fractionations associated with phosphoric acid digestion of carbonate minerals: insights from first-principles theoretical modeling and clumped isotope measurements. Geochim. Cosmochim. Acta 73, 7203–7225.

Hardie, L.A., 1996. Secular variation in seawater chemistry: an explanation for the coupled secular variation in the mineralogies of marine limestones and potash evaporates over the past 600 m.y. Geology 24, 279–283.

Holland, H.D., Horita, J., Seyfried, W., 1996. On the secular variations in the composition of Phanerozoic marine potash evaporates. Geology 24, 993–996.

Honlet, R., Gasparrini, M., Muchez, P., Swennen, R., John, C.M., 2017. A new approach to geobarometry by combining fluid inclusion and clumped isotope thermometry in hydrothermal carbonates. Terra Nova 30, 199–206.

Hood, A.vS., Wallace, M.W., 2012. Synsedimentary diagenesis in a Cryogenian reef complex: ubiquitous marine dolomite precipitation. Sediment. Geol. 255-256, 56–71.

Hood, A.vS., Wallace, M.W., Drysdale, R.N., 2011. Neoproterozoic aragonite-dolomite seas? Widespread marine dolomite precipitation in Cryogenian reef complexes. Geology 39, 871–874.

Horita, J., 2014. Oxygen and carbon isotope fractionation in the system dolomite-water-CO_2 to elevated temperatures. Geochim. Cosmochim. Acta 129, 111–124.

Hu, B., Radke, J., Schlüter, H.-J., Heine, F.T., Zhou, L., Bernasconi, S.M., 2014. A modified procedure for gas-source isotope ratio mass spectrometry: the long-integration dual-inlet (LIDI) methodology and implications for clumped isotope measurements. Rapid Commun. Mass Spectrom. 28, 1413–1425.

Huang, S., Huang, K., Lü, J., Lan, Y., 2014. The relationship between dolomite textures and their formation temperature: a case study from the Permian-Triassic of the Sichuan Basin and the Lower Paleozoic of the Tarim Basin. Pet. Sci. 11, 39–51.

Illing, L.V., Wells, A.J., Taylor, J.C.M., 1965. Penecontemporaneous dolomite in the Persian Gulf. In: Pray, L.C., Murray, R.C. (Eds.), Dolomitization and Limestone Diagenesis. Special Publication-*Society of Economic Paleontologists and Mineralogists*, vol. 13. pp. 89–111.

John, C.M., Bowen, D., 2016. Community software for challenging isotope analysis: first applications of "Easotope" to clumped isotopes. Rapid Commun. Mass Spectrom. 30, 2285–2300.

Kaczmarek, E.S., Thornton, B.P., 2017. The effect of temperature, cation ordering, and reaction rate in high-temperature dolomitization experiments. Chem. Geol. 468, 32–41.

Kele, S., Breitenbach, S.F.M., Capezzuoli, E., Meckler, A.N., Ziegler, M., Millan, I.M., Kluge, T., Deák, J., Hanselmann, K., John, C.M., Yan, H., Liu, Z., Bernasconi, S.M., 2015. Temperature dependence of oxygen- and clumped isotope fractionation in carbonates: a study of travertines and tufas in the 6-95 °C temperature range. Geochim. Cosmochim. Acta 168, 172–192.

Kelson, J.R., Huntington, K.W., Schauer, A.J., Saenger, C., Lechler, A.R., 2017. Towards a universal carbonate clumped isotope calibration: diverse synthesis and preparatory methods suggest a single temperature relationship. Geochim. Cosmochim. Acta 197, 104–131.

Kluge, T., John, C.M., Jourdan, A.-L., Davis, S., Crawshaw, J., 2015. Laboratory calibration of the calcium carbonate clumped isotope thermometer in the 25-250 °C temperature range. Geochim. Cosmochim. Acta 157, 213–227.

Land, L.S., 1980. The isotopic and trace element geochemistry of dolomite: the state of the art. In: Zenger, D.H., Dunham, J.B., Ethington, R.L. (Eds.), Concepts and Models of Dolomitization. Spec. Publ. –*SEPM*. vol. 28. pp. 87–110.

Land, L.S., 1985. The origin of massive dolomite. J. Geol. Educ. 33, 112–125.

Land, L.S., 1998. Failure to precipitate dolomite at 25 degrees C from dilute solution despite 1000-fold oversaturation after 32 years. Aquat. Geochem. 4, 361–368.

Lehner, P., 1952. Zur Geologie des Gebietes der Denti della Vecchia, des M. Boglia, des M. Brè, und des Monte Salvatore bei Lugano. Eclogae Geol. Helv. 45, 86–159.

Leutert, T.J., Sexton, P.F., Tripati, A., Piasecki, A., Ho, S.L., Meckler, A.N., 2019. Sensitivity of clumped isotope temperatures in fossil benthic and planktic foraminifera to diagenetic alteration. Geochim. Cosmochim. Acta 257, 354–372.

Lloyd, M.K., Eiler, J.M., Nabelek, P.I., 2017. Clumped isotope thermometry of calcite and dolomite in a contact metamorphic environment. Geochim. Cosmochim. Acta 197, 323–344.

Lloyd, M.K., Ryb, U., Eiler, J.M., 2018. Experimental calibration of clumped isotope reordering in dolomite. Geochim. Cosmochim. Acta 242, 1–20.

Lumsden, D.N., Chimahusky, J.S., 1980. Relationship between dolomite non-stoichiometry and carbonate facies parameters. SEPM 28, 123–137.

Mangenot, X., Gasparrini, M., Rouchon, V., Bonifacie, M., 2018. Basin-scale thermal and fluid flow histories revealed by carbonate clumped isotopes (Δ_{47}) – Middle Jurassic carbonates of the Paris Basin depocentre. Sedimentology 65, 123–150.

Matthews, A., Katz, A., 1977. Oxygen isotope fractionation during the dolomitization of calcium carbonate. Geochim. Cosmochim. Acta 41, 1431–1438.

McCormack, J., Bontognali, T.R.R., Immenhauser, A., Kwiecien, O., 2018. Controls on cyclic formation of Quaternary early diagenetic dolomite. Geophys. Res. Lett. 45, 3625–3634.

Meckler, A.N., Ziegler, M., Millán, M.I., Breitenbach, S.F.M., Bernasconi, S.M., 2014. Long-term performance of the Kiel carbonate device with a new correction scheme for clumped isotope measurements. Rapid Commun. Mass Spectrom. 28, 1705–1715.

Millán, I.M., Machel, H.G., Bernasconi, S.M., 2016. Constraining temperatures of formation and composition of dolomitizing fluids in the Upper Devonian Nisku Formation (Alberta, Canada) with clumped isotopes. J. Sediment. Res. 86, 107–112.

Müller, I.A., Violay, M.E.S., Storck, J.C., Fernandez, A., van Dijk, J., Madonna, C., Bernasconi, S.M., 2017a. Clumped isotope fractionation during phosphoric acid digestion of carbonates at 70 °C. Chem. Geol. 449, 1–14.

Müller, I.A., Fernández, A., Radke, J., van Dijk, J., Bowen, D., Schwieters, J., Bernasconi, S., 2017b. Carbonate clumped isotope analyses with the long-integration dual-inlet (LIDI) workflow: scratching at the lower sample weight boundaries. Rapid Commun. Mass Spectrom. 31, 1057–1066.

Murray, S.T., Swart, P.K., 2017. Evaluating formation fluid models and calibrations using clumped isotope paleothermometry on Bahamian dolomites. Geochim. Cosmochim. Acta 206, 73–93.

Murray, S.T., Arienzo, M.M., Swart, P.K., 2016. Determining the Δ_{47} acid fractionation in dolomites. Geochim. Cosmochim. Acta 174, 42–53.

Northrop, D.A., Clayton, R.N., 1966. Oxygen-isotope fractionations in systems containing dolomite. J. Geol. 74, 174–196.

Passey, B.H., Levin, N.E., Cerling, T.E., Brown, F.H., Eiler, J.M., 2010. High-temperature environments of human evolution in East Africa based on bond ordering in paleosol carbonates. PNAS 107, 11245–11249.

Peral, M., Daëron, M., Blamart, D., Bassinot, F., Dewilde, F., Smialkowski, N., Isguder, G., Bonnin, J., Jorissen, F., Kissel, C., Michel, E., Vázquez Riveiros, N., Waelbroeck, C., 2018. Updated calibration of the clumped isotope thermometer in planktonic and benthic foraminifera. Geochim. Cosmochim. Acta 239, 1–16.

Petersen, S.V., Defliese, W.F., Saenger, C., Daëron, M., Huntington, K.W., John, C.M., Kelson, J.R., Bernasconi, S.M., Coleman, A.S., Kluge, T., Olack, G.A., Schauer, A.J., Bajnai, D., Bonifacie, M., Breitenbach, S.F.M., Fiebig, J., Fernandez, A.B., Henkes, G.A., Hodell, D., Katz, A., Kele, S., Lohmann, K.C., Passey, B.H., Peral, M.Y., Petrizzo, D.A., Rosenheim, B.E., Tripati, A., Venturelli, R., Young, E.D., Winkelstern, I.Z., 2019. Effects of improved ^{17}O correction on inter-laboratory agreement in clumped isotope calibrations, estimates of mineral-specific offsets, and temperature dependence of acid digestion fractionation. Geochem. Geophys. Geosyst. https://doi.org/10.1029/2018GC008127.

Piasecki, A., Bernasconi, S.M., Grauel, A., Hannisdal, B., Ho, S.L., Leutert, T.J., Marchitto, T.M., Meinicke, N., Tisserand, A., Meckler, N., 2019. Application of clumped isotope thermometry to benthic foraminifera. Geochem. Geophys. Geosyst. 40, 2082–2090.

Preto, N., Breda, A., dal Corso, J., Spötl, C., Zorzi, F., Frisia, S., 2015. Primary dolomite in the Late Triassic Travenanzes Formation, Dolomites, Northern Italy: facies control and possible bacterial influence. Sedimentology 62, 697–716.

Rodriguez-Blanco, J.D., Shaw, S., Benning, L.G., 2015. A route for the direct crystallization of dolomite. Am. Mineral. 100, 1172–1181.

Rodríguez-Sanz, L., Bernasconi, S.M., Marino, G., Heslop, D., Müller, I.A., Fernandez, A., Grant, K.M., Rohling, E.J., 2017. Penultimate deglacial warming across the Mediterranean Sea revealed by clumped isotopes in foraminifera. Sci. Rep. 7 (16572), 1–11.

Rosenbaum, J., Sheppard, S.M., 1986. An isotopic study of siderites, dolomites and ankerites at high temperatures. Geochim. Cosmochim. Acta 50, 1147–1150.

Ryb, U., Lloyd, M.K., Stolper, D.A., Eiler, J.M., 2017. The clumped-isotope geochemistry of exhumed marbles from Naxos, Greece. Earth Planet. Sci. Lett. 470, 1–12.

Schmid, T.W., Bernasconi, S.M., 2010. An automated method for 'clumped-isotope' measurements on small carbonate samples. Rapid Commun. Mass Spectrom. 24, 1955–1963.

Sharma, T., Clayton, R.N., 1965. Measurement of O^{18}/O^{16} ratios of total oxygen of carbonates. Geochim. Cosmochim. Acta 29, 1347–1353.

Smeraglia, L., Bernasconi, S.M., Berra, F., Billi, A., Boschi, C., Caracausi, A., Carminati, E., Castorina, F., Doglioni, C., Italiano, F., Rizzo, A.L., Uysal, I.T., Zhao, J.-X., 2018. Crustal-scale fluid circulation and co-seismic shallow comb-veining along the longest normal fault of the central Apennines, Italy. Earth Planet. Sci. Lett. 498, 152–168.

Spencer, R.J., Hardie, L.A., 1990. Control of seawater composition by mixing of river waters and mid-ocean ridge hydrothermal brines. In: Spencer, R.J., Chou, I.M. (Eds.), Fluid Mineral Interactions: A Tribute to H.P. Eugster. vol. 2. Geochemical Society Special Publication, pp. 409–419.

Suarez, M.B., Ludvigson, G.A., González, L.A., You, H.-L., 2017. Continental

paleotemperatures from an Early Cretaceous dolomitic Lake, Gansu Province, China. J. Sediment. Res. 87, 486–499.

van Dijk, J., Fernandez, A., Storck, J.C., White, T.S., Lever, M., Müller, I.A., Bishop, S., Seifert, R.F., Driese, S.G., Krylov, A., Ludvigson, G.A., Turchyn, A.V., Lin, C.Y., Wittkop, C., Bernasconi, S.M., 2019. Experimental calibration of clumped isotopes in siderite between 8.5 and 62 °C and its application as paleo-thermometer in paleosols. Geochim. Cosmochim. Acta 254, 1–20.

Van Lith, Y., Vasconcelos, C., Warthmann, R., Martins, J.C.F., McKenzie, J.A., 2002. Bacterial sulfate reduction and salinity: two controls on dolomite precipitation in Lagoa Vermelha and Brejo do Espinho (Brazil). Hydrobiologia 485, 35–49.

Vasconcelos, C., McKenzie, J.A., 1997. Microbial mediation of modern dolomite precipitation and diagenesis under anoxic conditions (Lagoa Vermelha, Rio de Janeiro, Brazil). J. Sediment. Res. 67, 378–390.

Vasconcelos, C., McKenzie, J.A., Warthmann, R., Bernasconi, S.M., 2005. Calibration of the $\delta^{18}O$ paleothermometer for dolomite precipitated in microbial cultures and natural environments. Geology 33, 317–320.

Wacker, U., Fiebig, J., Schoene, B.R., 2013. Clumped isotope analysis of carbonates: comparison of two different acid digestion techniques. Rapid Commun. Mass Spectrom. 27, 1631–1642.

Warren, J., 2000. Dolomite: occurrence, evolution and economically important associations. Earth Sci. Rev. 52, 1–81.

Wilson, E.N., Hardie, L.A., Phillips, O.M., 1990. Dolomitization front geometry, fluid flow patterns, and the origin of massive dolomite: the Triassic Latemar buildup, Northern Italy. Am. J. Sci. 290, 741–796.

Winkelstern, I.Z., Lohmann, K.C., 2016. Shallow burial alteration of dolomite and limestone clumped isotope geochemistry. Geology 44, 463–466.

Winkelstern, I.Z., Kaczmarek, S.E., Lohmann, K.C., Humphrey, J.D., 2016. Calibration of dolomite clumped isotope thermometry. Chem. Geol. 443, 32–38.

Wright, D.T., 1997. An organogenic origin for widespread dolomite in the Cambrian Eilean Dubh Formation, northwestern Scotland. J. Sediment. Res. 67, 54–64.

Wright, D.T., 1999. The role of sulphate-reducing bacteria and cyanobacteria in dolomite formation in distal ephemeral lakes of the Coorong region, South Australia. Sediment. Geol. 126, 147–157.

Zaarur, S., Affek, H.P., Brandon, M.T., 2013. A revised calibration of the clumped isotope thermometer. Earth Planet. Sci. Lett. 382, 47–57.

Zar, J., 1984. Biostatistical Analysis, 2nd ed. Prentice-Hall Chapter 18.

Zheng, Y.-F., 1999. Oxygen isotope fractionation in carbonate and sulfate minerals. Geochem. J. 33, 109–126.

Zorn, H., 1971. Paläontologische, stratigraphische und sedimentologische Untersuchungen des Salvatoredolomits (Mitteltrias) der Tessiner Kalkalpen. In: Kuhn-Schnyder, E., Peyer, B. (Eds.), Die Triasfauna der Tessiner Kalkalpen. XXI. *Schweizerische Paläontologische Abhandlungen.* vol. 91. pp. 1–90.